Mapping the age of the subducting Pacific slab beneath East Asia

*Dapeng Zhao[1], Xin Liu[2], S. Li[2], W. Wei[3]

1. Department of Geophysics, Tohoku University, 2. Ocean University of China, 3. China Earthquake Administration

We map the age of the subducting Pacific slab beneath East Asia using a high-resolution model of P-wave tomography and paleo-age data of ancient seafloor. Our results show that the subducting oceanic lithosphere becomes younger from the Japan Trench (~130 Ma) to the slab' s western tip (~90 Ma) beneath East Asia. Such a feature indicates that the flat (stagnant) slab now in the mantle transition zone (MTZ) beneath East Asia is the subducted Pacific slab rather than the Izanagi slab which should have already sunk into the lower mantle. The subduction age of the Pacific slab ranges from 0 Ma at the present-day trench to ~30 Ma at the western tip of the flat slab in the MTZ beneath central China. The stagnant duration of the flat Pacific slab in the MTZ is no more than ~10-20 million years, much shorter than the age of the big mantle wedge (BMW) beneath East Asia (>110 million years). It is the present Pacific slab that has contributed to the Cenozoic lithosphere destruction, extensive intraplate volcanism, and back-arc spreading in East Asia, whereas the destruction of the North China Craton during the Early Cretaceous (~140-110 Ma) was caused by the subduction of the Izanagi (or the Paleo-Pacific) plate.

Keywords: Slab age, Pacific plate, East Asia

Mantle convection: clues from lithosphere sinking at subduction zones and numerical modelling.

*Eleonora Ficini[1], Marco Cuffaro[2], Carlo Doglioni[1,3]

1. Sapienza Univ., 2. IGAG-CNR, 3. INGV

Subduction zones show a worldwide asymmetry that can be observed in slab dip, kinematics of the subduction hinge, morphology, structural elevation, gravity anomalies, heat flow, metamorphic evolution, subsidence and uplift rates, depth of the decollement planes, mantle wedge thickness, magmatism, backarc development or not, etc. This asymmetry could be easily explained if related to the geographic polarity of the sinking slabs (Doglioni & Panza, 2015). In fact, geophysical and kinematics constraints show that all the plates move “westward”. This preferential flow of plates would suggest a relative “eastward” mantle flow. If we look then to subduction dynamics within this set of conditions, this “eastward” mantle flow should have an important role in influencing subduction dynamics itself. Furthermore, along W-subduction zones slabs sink with a higher velocity with respect to the “easterly or northeasterly” directed ones. The faster “westerly” directed slabs determine that the volume of lithosphere recycled into this kind of subduction is larger than that along the converse ones. This should determine a more vigorous counterflow within the mantle below W-directed subductions with respect to the one below E-directed ones. Starting from these observations we attempted to estimate volumes of lithosphere that are currently subducting below the principal subduction zones: our results show that there are about 288 km^3/yr of lithosphere currently subducting below W-directed subduction zones, while only about 78 km^3/yr of lithosphere are currently subducting below E- to NE-directed subduction zones. Then we tried to demonstrate quantitatively the consequent difference in mantle circulation between the two subduction settings using numerical modelling tools (Gerya, 2010), using data coming from our volumetric calculation as input data for the models. Moreover, we tried to look at these volumes with respect to the latitude of subduction zones, being plates velocities strongly linked to the Earth’s rotation. In fact, seismicity is latitude dependent and decreases with increasing latitude (Riguzzi *et al.*, 2010; Varga *et al.*, 2012). Our results show that most of the volume currently subducting below worldwide principal subduction zones is concentrated between 30° and -30° of latitude.

References

Doglioni C. & Panza G. Polarized Plate Tectonics. Adv. Geophys., 56, 1-167 (2015).
Gerya, T. Introduction to Numerical Geodynamic Modelling, Cambridge University Press (2010).
Riguzzi F., Panza G., Varga P. & Doglioni C. Can Earth’s rotation and tidal despinning drive plate tectonics? Tectonophysics, 484, 60-73 (2010).
Varga P., Krumm F., Riguzzi F., Doglioni C., Süle B., Wang K. & Panza G. F. Global pattern of earthquakes and seismic energy distributions: Insights for the mechanisms of plate tectonics. Tectonophysics, 530-531, 80-86 (2012).

Keywords: subduction, mantle convection

Quasi-3D seismological imaging of Caroline plate using Monte-Carlo waveform inversion of teleseismic SS phases

*Hyoihn Jang[2], Nobuaki Fuji[1], David Fernández-Blanco[1], Younghee Kim[2], Kensuke Konishi[3], Sang-Mook Lee[2], Shihao Yuan[1]

1. Institut de Physique du Globe de Paris, 2. Seoul National University, 3. Academia Sinica

We present a quasi-3D S-wave velocity structure of the upper mantle under Southwest Pacific. Since it is fully covered by the ocean, seismic station coverage in this region is poor, leading a poorer resolution with respect to other regions in previous global tomographic studies. We collect 126 seismic events recorded at 35 AU stations, resulting a dataset of > 4200 pairs of event and station. In order to obtain a high resolving power, we use SS phases that have their bouncing points in the vicinity of the region. We perform regional 1D Monte Carlo waveform inversion using a combination of waveform and traveltime residuals between observed and synthetic data as a cost function. We generate 10.000 1D models for each pair of event and station and each pair chooses its preferred models that minimize the misfit function as a combination of SS-S traveltime double differences and SS waveform residuals. The mantle transition zone beneath the Caroline plate shows 1-3 % higher Vs anomaly with respect to PREM but the anomaly is cutted vertically by a low velocity zone (~1-2 % lower to PREM) underneath the Eauripik Rise which is situated in the center of Caroline plate. This low velocity zone can be interpreted as a thin plume coming from the base of the mantle, which could be locked due to the complex tectonics in the shallower part.

Keywords: Caroline plate, Monte-Carlo inversion, waveform inversion

Effects of rheological parameters on continental drift and water cycling in 3D mantle convection

*Ryunosuke Yanagi[1], Masaki Yoshida[2], Hikaru Iwamori[1,2]

1. Tokyo Institute of Technology, 2. Japan Agency for Marine-Earth Science and Technology

The Earth is unique among the solar terrestrial planets, having the continents and the abundant liquid water on its surface. From some previous studies (e.g., Iwamori and Nakamura, 2015, Gondwana Res.; Yanagi et al., 2016, Abstr. of JpGU Meeting), it has been thought that the continental dispersal and coalescence are in a close relationship with water distribution in the mantle. However, there are some problems for reproducing continental dispersal and coalescence. One of the fundamental problems concerns the mechanism of continental dispersal and coalescence. For instance, we do not know when and how the continent would be broken up. In this study, we have varied the values of a yield stress of the lithosphere and an activation energy of the mantle rock, which are thought to be key parameters for mantle convection. The reason we selected these two parameters is that yield stress controls the vulnerability of lithosphere and the activation energy is related to viscosity variation in the mantle, both of which affect the pattern of the continental dispersal and coalescence. The model used in this study is a three-dimensional (3-D) mantle convection model incorporating presence of the continental materials. In this numerical simulation of 3-D spherical mantle convection, the supercontinent is introduced in the initial state of the simulation run in order to study how continental dispersal and coalescence occurs and affect the structure of the Earth’ s interior. This study will test a hypothesis that there is a close relationship between the mechanisms of continental drift and the lithospheric conditions that depend on the yield stress and the activation energy. In addition, the water solubility of the mantle rock is considered in this model for understanding the effect of continental drift on water transportation in the mantle. Our studies will also examine global structures for water distribution in the mantle as proposed by Iwamori and Nakamura (2015) and Yanagi et al. (2016).

Keywords: three-dimensional mantle convection, continental dispersal and coalescence, water cycling, yield stress, viscosity

Uppermost mantle Pn tomography with Moho depth correction from eastern Europe to western China

*Yan Lyu[1], Sidao Ni[2], Ling Chen[3], Qi-Fu Chen[1]

1. Key Laboratory of Earth and Planetary Physics, Institute of Geology and Geophysics, Chinese Academy of Sciences, Beijing 100029, China, 2. State Key Laboratory of Geodesy and Earth's Dynamics, Institute of Geodesy and Geophysics, Chinese Academy of Sciences, Wuhan 430077, China, 3. State Key Laboratory of Lithospheric Evolution, Institute of Geology and Geophysics, Chinese Academy of Sciences, Beijing 100029, China

We proposed a modified Pn velocity and anisotropy tomography method by considering the Moho depth variations using the Crust 1.0 model and obtained high-resolution images of the uppermost mantle Pn velocity and anisotropy structure from eastern Europe to western China. The tomography results indicate that the average Pn velocities are approximately 8.0 and 8.1 km/s under the western and eastern parts of the study area, respectively, with maximum velocity perturbations of 3%–4%. We observed high Pn velocities under the Adriatic Sea, Black Sea, Caspian Sea, Arabian Plate, Indian Plate, and in the Tarim and Sichuan basins but low Pn velocities under the Apennine Peninsula, Dead Sea fault zone, Anatolia, Caucasus, Iranian Plateau, Hindu Kush, and in the Yunnan and Myanmar regions. Generally, regions with stable structures and low lithospheric temperatures exhibit high Pn velocities. Low Pn velocities provide evidence for the upwelling of hot material, which is associated with plate subduction and continental collision processes. The Pn anisotropy structure reflects the stress state of the uppermost mantle and indicates the location of the plate collision boundary at the depth of the Moho. Our Pn velocity and anisotropy imaging results indicate that the Adriatic microplate dives to the east and west, the hot material upwelling caused by subduction beneath the Tibetan Plateau is not as significant as that in the Caucasus and Myanmar regions, the lithosphere exhibits coupled rotational movement around the Eastern Himalayan Syntaxes, and the areas to the north and south of 26°N in the Yunnan region are affected by different geodynamic processes. Our newly captured images of the uppermost mantle velocity and anisotropy structure provide further information about continental collision processes and associated dynamic mechanisms.

Keywords: uppermost mantle, Pn, velocity, anisotropy

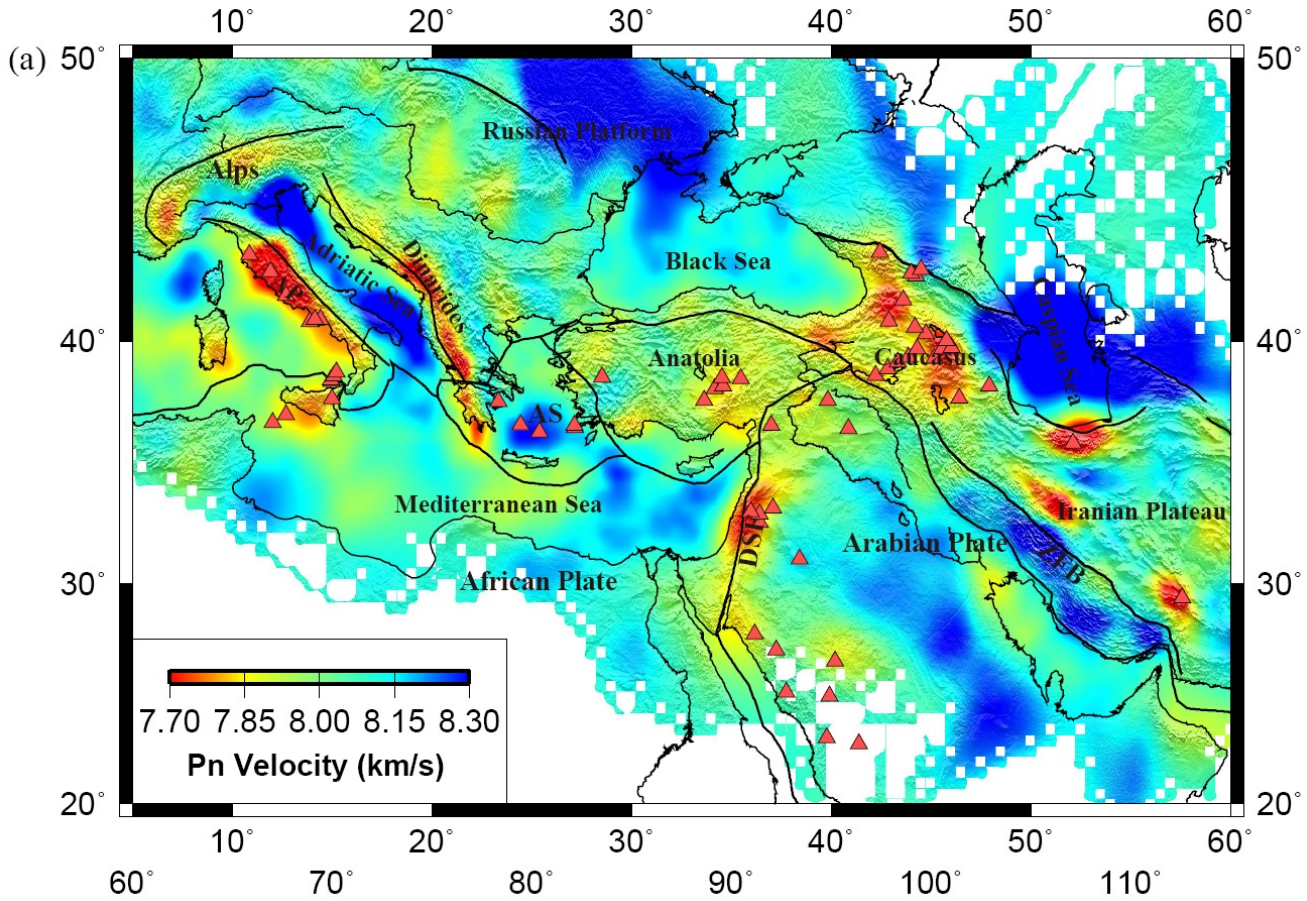

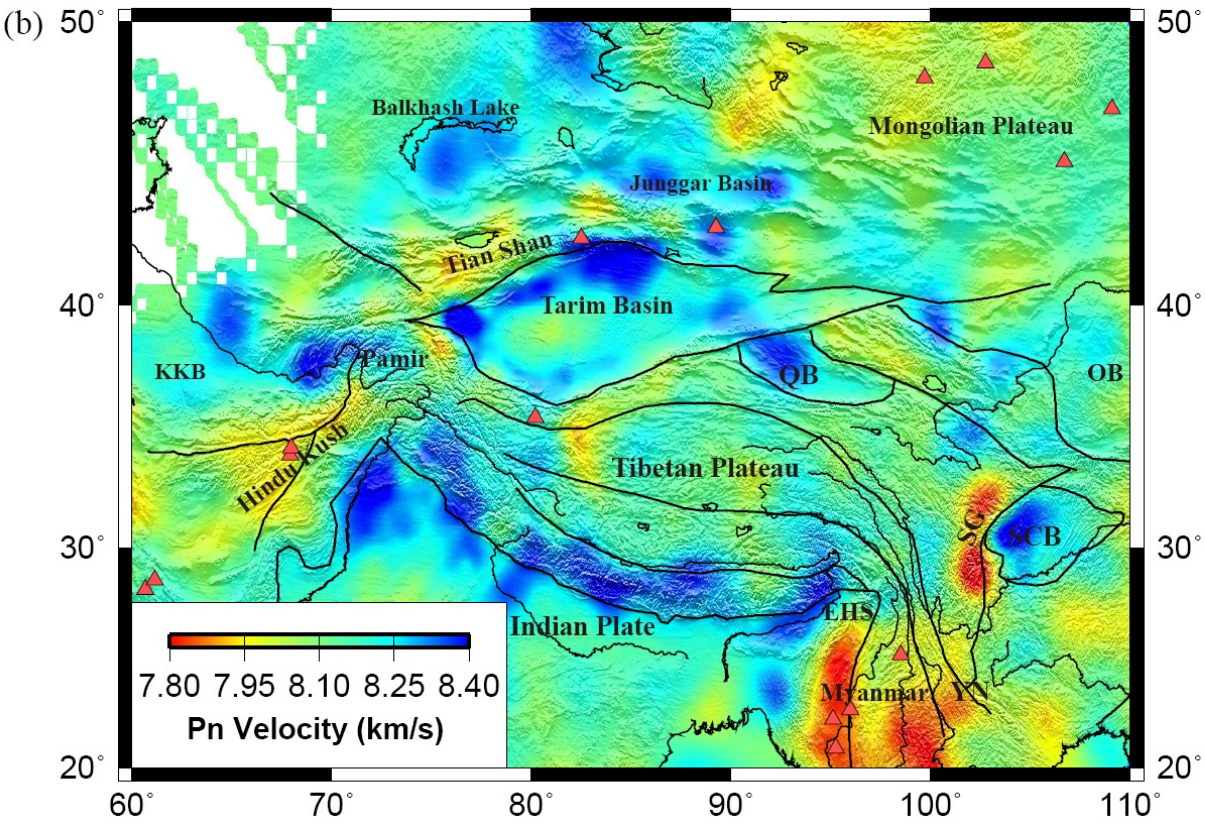

Azimuthal anisotropy of Rayleigh-wave phase velocities in Cameroon, West Africa.

*Adebayo Oluwaseun Ojo[1], Sidao Ni[2], Haopeng Chen[2]

1. School of Earth and Space Sciences, University of Science and Technology of China, Hefei, 230026, China; Department of Geosciences, Faculty of Science, University of Lagos, Akoka-Yaba, Lagos, Nigeria, 2. State Key Laboratory of Geodesy and Earth's Dynamics, Institute of Geodesy and Geophysics, Chinese Academy of Sciences, Wuhan, 430077, China

The Cameroon region contains several tectonic features of interest to earth scientists. One of these is a chain of intra-plate volcanic line (CVL) without age progression. Since the CVL defies common geodynamic explanations, its origin has been subjected to considerable debate without reaching a consensus. Therefore, to advance understanding of the deformation and flow patterns resulting from the CVL and other tectonic processes in Cameroon, we imaged the azimuthal anisotropy of Rayleigh wave phase velocities from 4 to 60 seconds.

The seismic data used for this study was retrieved from both ambient seismic noise records and teleseismic earthquake data recorded by 32 broadband seismic stations deployed during the lifetime of the Cameroon Broadband Seismic Experiment (CBSE). First, we analyzed vertical component seismograms for 310 earthquakes with magnitude 5.0 occurring between the distances of 30^0 to 90^0. The traditional two-station method is adopted for measuring the inter-station phase velocities. Secondly, we processed continuous records of ambient seismic noise data from January to December 2006 following the method detailed in Ojo et al. (2017). For each inter-station path, we measured the phase velocity using the frequency-time analysis method. Following Yao et al. (2008), we averaged the dispersion from both datasets for similar station pairs by effectively weighting up earthquake measurements at long periods and ambient noise measurements at short periods. We eliminated erroneous phase velocity data that lay outside 2 σ and those that did not meet the one wavelength criteria. Finally, we used the continuous Tarantola inversion program to obtain 2-D isotropic phase velocity and azimuthal anisotropy (amplitude and fast direction) maps from the path-averaged dispersion at each period.

The results revealed an obvious stratified azimuthal anisotropy beneath the Adamawa Plateau and Garuoa Rift (Northern part of CVL). The fast direction changes from NE–SW in the period band of 4-30s to NW-SE at longer periods which correspond to deeper depths. The distinct pattern of azimuthal anisotropy at short and long periods implies that the deformation varies with depth. Hence, we proposed a layered mechanism of deformation with almost independent processes at shorter and longer periods resulting from both frozen-in and present sources. This may also reflect decoupling of deformation or successive deformation episodes recorded at different depths. A consistent NE-SW fast direction is found at most period band beneath the Congo Craton. However, at around 38-44s a transition zone (probably indicative of the Moho) with N-S fast direction is revealed. This observation suggests a frozen-in anisotropy related to the NE-ward movement of the asthenosphere relative to the African plate. Along the southern part of the CVL, the fast direction trends N-S at short periods and changes to NNE-SSW at longer periods. We interpret this as first-order evidence for dominated northward and upward flow of plume materials associated with magma intrusion. The direction of fast axis beneath the Oubanguides Belt is largely NE-SW. This direction is parallel to the strike direction of known strike-slip faults in the study area, suggesting a lithospheric origin for the observed azimuthal anisotropy.

Our results provide new evidence for the existence of small-scale convection in the asthenosphere related to the formation of the CVL and help constrain the source region of previous shear wave splitting studies in the study area.

References

Ojo, A. O., Ni, S. and Li, Z., 2017. Crustal radial anisotropy beneath Cameroon from ambient noise tomography. Tectonophysics 696–697, 37–51.

Yao, H., Beghein, C., and Van der Hilst, R.D., 2008. Surface-wave array tomography in SE Tibet from ambient seismic noise and two-station analysis: II - Crustal and upper mantle structure. Geophys. J. Int., 173 (1), 205-219.

Keywords: Azimuthal Anisotropy, Cameroon, Surface waves

Electrical conductivity as a constraint on lower mantle thermo-chemical structure

*Frederic Deschamps[1], Amir Khan[2]

1. Academia Sinica, 2. ETH Zurich

Electrical conductivity of the Earth’ s mantle depends on both temperature and compositional parameters, and radial and lateral variations in conductivity are thus potentially a powerful means to investigate its thermo-chemical structure. Here, we use available electrical conductivity data for the major lower mantle minerals, bridgmanite and ferropericlase, to calculate 3D maps of lower mantle electrical conductivity for two possible models: a purely thermal model, and a thermo-chemical model. Both models derive from probabilistic seismic tomography, and the thermo-chemical model includes, in addition to temperature anomalies, variations in volume fraction of bridgmanite and iron content. The electrical conductivity maps predicted by these two models are clearly different. Compared to the purely thermal model, the thermo-chemical model leads to higher electrical conductivity, by about a factor 2.5, and stronger lateral anomalies. In the lowermost mantle (2000-2891 km) the thermo-chemical model results in a belt of high conductivity around the equator, whose maximum value reaches ~120% of the laterally-averaged value and is located in the low shear-wave velocity provinces imaged in tomographic models. Based on our electrical conductivity maps, we computed electromagnetic response function (C-responses) and found, again, strong differences between the C-responses for purely thermal and thermo-chemical models. At periods of 1 year and longer, C-responses based on thermal and thermo-chemical models are easily distinguishable. Furthermore, C-responses for thermo-chemical model vary geographically. Our results therefore show that long-period (1 year and more) variations of the magnetic field may provide key insights on the nature and structure of the deep mantle.

Keywords: Mantle structure, Electrical conductivity, Electromagnetic C-response

The effect of iron on the elastic properties of wadsleyite at the transition zone condition

*Wei Sun[1], Steeve Gréaux [1], Tetsuo Irifune[1]

1. Geodynamics Research Center, 2-5 Bunkyo-cho, Matsuyama, Ehime 790-8577, Japan.

Wadsleyite is believed to be the major component in the upper part of the transition zone. To interpret seismic models in terms of mineralogy and chemical composition, the elastic bulk and shear moduli of wadsleyite and its derivatives as a function of pressure, temperature and Fe concentration are the critical parameters in extrapolating laboratory results to mantle conditions. However, former studies [ex. *Liu et al.* , 2009] on wadsleyite were performed at low pressure (<12 GPa) and temperature (<1100 K) and their extrapolations to the seismic models in transition zone condition are difficult because derivatives of the elastic moduli function to pressure and temperature are non-linear. On the other hand, Fe effect on the seismic velocities has never been systemically studied and poorly constrained.
In this study, we employed ultrasonic method combined with multi-anvil apparatus and in-situ X-ray observations developed by *Higo et al.* [2008] to investigate the elastic properties of wadsleyite at high temperature and pressure. The elastic bulk and shear moduli with diverse Fe concentration (Fe#=0 and 10) have been determined up to 1700K and 20 GPa. Based on our results, derivatives of seismic velocities observed among locations at the transition zone depth could be explained by Fe content variation in wadsleyite except the wedge mantle, which is consistent with the conclusion from electrical conductivities [*Yoshino et al.*, 2009].

Keywords: wadsleyite, elastic properties, the transition zone

The relationship between creep and grain growth rates in forsterite+periclase polycrystals

*Atsuro Okamoto[1], Takehiko Hiraga[1]

1. Earthquake Research Institute, The University of Tokyo

Absence of seismic anisotropy in the earth's lower mantle suggests deformation by diffusion creep mechanism (Karato et al., 1995). The mantle is considered to consist mainly of perovskite and ferropericlase. Thus, it is required to understand a mechanism of diffusion creep of a two-phase material. The diffusion creep is significantly sensitive to grain size such that the flow in the lower mantle is likely to be controlled by grain growth (Solomatov, 1996). Both creep and grain growth require diffusion of atoms with a long-distance, which is almost the size of grains. Thus, it is likely that rate-controlling processes for creep and grain growth are identical. To examine this prediction, we conducted creep and grain growth experiments on an analogue material of the lower mantle, which consists of elements similar to the lower mantle minerals, at high-temperature and atmospheric pressure.
We synthesized highly-dense forsterite + periclase (10vol%) polycrystals from a mixture of fine powders of $Mg(OH)_2$ and SiO_2 (Koizumi et al., 2010). Grain sizes of forsterite and periclase are 0.3 and 0.2 μm, respectively. We performed uni-axial compressional creep experiments on these materials at atmospheric pressure. Prior to the deformation, the sample was annealed at 1420℃ for 12h to avoid grain growth during the experiment. We changed loads ranging from 50 to 200 MPa under constant temperatures of 1180℃~1400℃ during the experiments. At each stress level, we measured a strain rate where we could assume steady-state creep. We also performed grain growth experiments at different temperatures ranging from 1280℃ to 1400℃ for 500h using temperature gradient formed outside the central heat zone in the furnace. We observed microstructures of the aggregates after the experiments using scanning electron microscope (SEM).
Based on creep data, we obtained a relationship of $d\varepsilon/dt \propto \sigma^n$ (n = 1.3~1.6). We observed monotonic increment of grain sizes of both forsterite and periclase grains with increasing temperature. We calculated grain boundary diffusivities from rates of creep and grain growth using theoretical models for grain growth and for diffusion creep (Coble creep), finding both diffusivities are essentially identical. The diffusivities are compared with previously measured grain boundary diffusivity of Si^{4+} (Fei et al., 2016) and MgO (Gardes & Heinrich, 2011) finding our values are comparable to the diffusivity of Si^{4+}. We will discuss the flow mechanism of the lower mantle based on these results.

Keywords: Rheology of the lower mantle, Diffusion creep of a two-phase material, Grain boundary diffusivity

Inversion of waveform data for radial profiles of shear velocity and attenuation of the lowermost mantle beneath the western Pacific

*Kensuke Konishi[1], Nobuaki Fuji[2], Frederic Deschamps[1]

1. Academia Sinica, 2. Institut de physique du globe de Paris

The existence of large low shear velocity provinces (LLSVPs) in the lowermost mantle is widely known by seismological global-scale studies. To understand the nature of these features, we investigate the elastic and anelastic structure of the lowermost mantle at the western edge of the Pacific LLSVP by inverting a collection of S and ScS waveforms. The transverse component data were obtained from F-net for 31 deep earthquakes beneath Tonga and Fiji, filtered between 12.5 and 200 s. We observe a regional variation of S and ScS arrival times and amplitude ratios, according to which we divide our region of interest into three subregions. For each of these subregions, we then perform 1D (depth-dependent) waveform inversions simultaneously for radial profiles of shear wave velocity (VS) and seismic quality factor (Q). In figure, models for all three subregions (#1-3) show low VS (a) and low Q (b) structures from 2000 km depth down to the core–mantle boundary. We further find that VS and Q in the central subregion, sampling the Caroline plume, are substantially lower than in the surrounding regions, whatever the depth. In the central subregion, VS-anomalies with respect to PREM (dVS) and Q are about −2.5 per cent and 216 at a depth of 2850 km, and −0.6 per cent and 263 at a depth of 2000 km. By contrast, in the two other regions, dVS and Q are −2.2 per cent and 261 at a depth of 2850 km, and −0.3 per cent and 291 at a depth of 2000 km. At depths greater than ˜2500 km, these differences may indicate lateral variations in temperature of ˜ 100 K within the Pacific LLSVP. At shallower depths, they may be due to temperature difference between the Caroline plume and its surroundings, and possibly to a small fraction of iron-rich material entrained by the plume.

Keywords: lowermost mantle, waveform inversion, anelastic structure

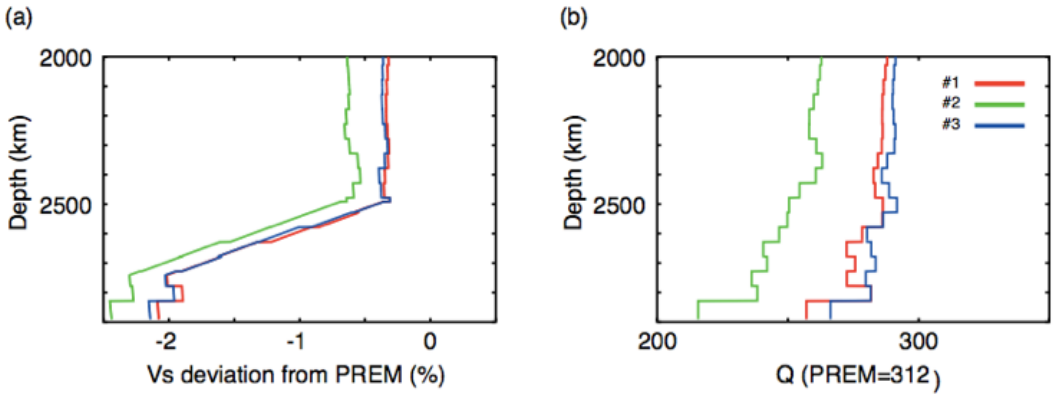

ab initio calculations reveal why thermal and compositional variations are required to explain observed mantle shear and compressional velocity anomalies

*Christine Houser[1], Renata Wentzcovitch[2], Juan Valencia-Cardona[3]

1. Earth-Life Science Institute, Tokyo Institute of Technology, 2. Columbia University, 3. University of Minnesota

The sensitivity of seismic velocity and density to composition and temperature determines the ability to detect changes in these properties in the lower mantle. We use recent ab initio calculations to predict the sensitivity of shear, bulk, and compressional velocity and density to changes in composition and temperature under lower mantle conditions. We calculate the predicted seismic signals for a suite of compositions and temperatures. These predictions are then compared to seismic tomography observations. If only shear velocities are used, the magnitude of observed seismic anomalies can be matched by varying temperature alone for any single composition. However, the compressional velocity sensitivity to temperature and composition is complex, in part due to the effects of the iron high spin to low spin transition in ferropericlase. We find it is essentially impossible to account for the observed magnitude of both shear and compressional velocities in a homogeneous mantle. Lateral and/or vertical gradients in composition are required to explain the fundamental properties of almost all joint tomography models.

Keywords: seismic tomography, mantle state and composition

Effect of pressure on temperature measurements using WRe thermocouple and its impact on geophysics

*Yu Nishihara[1], Shunta Doi[1], Sho Kakizawa[1], Yuji Higo[2], Yoshinori Tange[2], Tetsuo Irifune[1]

1. Geodynamics Research Center Ehime University, 2. Japan Synchrotron Radiation Research Institute

Our understanding of the Earth's interior highly depends on physical and chemical properties of the Earth materials which were determined based on high-pressure and high-temperature experiments. Temperature in these experiments is mostly determined using a thermocouple without any pressure correction. This may lead to erroneous results in estimated temperature and thus physical and chemical properties of the Earth materials due to significant pressure effects of the thermocouple electromotive force (EMF). However, knowledge of the absolute pressure effect on the EMF has been limited to relatively low pressures (<3.5 GPa) for more than 40 years (Getting and Kennedy, 1970).
Recently, we have developed a new method to determine the absolute pressure effect on thermocouple EMF at higher pressures based on a single wire method using Kawai-type multi-anvil apparatus (Nishihara et al., 2016). In this method, testing wires are subjected to higher and lower pressures by containing them in semi-sintered MgO and dense Al_2O_3 insulating tubes, respectively. The temperature along the single wires is calibrated by separate experiments employing multiple thermocouples. Pressure conditions along the wires are evaluated based on in situ X-ray diffraction using synchrotron X-ray radiation and their thermal equations of state. The pressure effect of the Seebeck coefficients is determined by the analyses of single wire EMFs and pressure-temperature profiles along the wires.
Based on this method, we have measured pressure effect on the EMF of W3Re-W25Re (type D) thermocouple up to 16 GPa and 900˚C. The difference of the nominal temperature from the real temperature was calculated to be −27˚C at 16 GPa and 900˚C. This absolute temperature correction may be underestimated due to influence of uniaxial stress during measurements. An extrapolation of the raw results suggest the temperature difference of −70˚C at 23 GPa and 1500˚C. *P-T* condition of the post-spinel phase boundary in Mg_2SiO_4 determined using type D thermocouple (Irifune et al., 1998; Katsura ae al., 2003) shifts to higher pressure by 0.5–0.7 GPa when temperature values are corrected. This corresponds to 12–16 km change of depth of the 660 km discontinuity. The temperature correction also has significant influence on the activation volumes for thermally activated processes such as element diffusion and rheology. The real values of activation volume determined at 0–10 GPa and 1500˚C is calculated to be ~1.3 cm^3/mol higher than nominal values when they are determined by experiments using type D thermocouple and the activation energy is 500 kJ/mol. This means that element diffusion and rheology are getting more sluggish with increase of depth in the Earth's mantle than previously estimated.

Keywords: temperature measurement, high-pressure and high-temperature, thermocouple, 660 km discontinuity

Dynamics of the fault motion and the origin of the contrasting tectonic style on Earth and Venus

*Shun-ichiro Karato[1], Sylvain Barbot[2]

1. Yale University, Department of Geology and Geophysics, 2. Earth Observatory of Singapore, Nanyang Technology University

Earth is a unique terrestrial planet on which plate tectonics operates. On a similar terrestrial planet like Venus (~95 % size of Earth), there is no evidence for plate tectonics at least in the recent ~500 Myrs. Various models have been proposed to explain this enigmatic observation including the difference in the water content and/or in the surface temperature. However, none of the previous models provide satisfactory explanation because they invoke processes that have not been quantitatively explored in any detail. For instance, models invoking different water content are difficult to explain weakening of the deep portions of the Earth's oceanic lithosphere. Similarly, proposed mechanism of grain-size reduction cannot explain weak shallow lithosphere without requiring unreasonably small grain-size. Here we propose an alternative model to explain the Earth-Venus contrast based on the well-established experimental observations on the dynamics of fault motion. Unstable, accelerated fault motion, which occurs only below ~400°C in the crust and ~600°C in the mantle that leads to the reduction of friction coefficient by melting. Based on the laboratory data on high-velocity friction, we show that thermal weakening makes Earth's lithosphere weak enough to make plate tectonics possible. In contrast, this weakening process is prohibited by the high surface temperature (~470°C) on Venus keeping the Venusian lithosphere strong. In this model, the difference in the surface temperature leads to the different tectonic style between Earth and Venus through the difference in the degree of dynamic weakening of fault motion.

Keywords: faults, thermal weakening, plate tectonics, Earth-Venus contrast

Proton conduction in hydrous forsterite aggregate at different buffered (MgO or SiO_2) conditions

*Chengcheng Zhao[1], Takashi Yoshino [1]

1. Institute for Planetary Materials, Okayama University

Hydrogen in magnesium site is expected to be the most active type in dominating hydrogen lattice diffusion and thus proton conduction in nominally anhydrous minerals (NAMS) (e.g. olivine) in past decades. However, an unexpected small amount of hydrogen in magnesium site pointed out by a growing number of researchers put it into question (e.g. Ingrin et al., 2013; Xue et al., in press). Even if it is not that case, water effect on electrical conductivity quantified by total water content has been inaccurate given the hypothesis that hydrogen diffusion rate was site-specific in forsterite (Padron-Navarta et al., 2014). Therefore, a further evaluation on proton conduction in olivine is required. To clarify the contribution of hydrogen in different sites, we measured the electrical conductivity of hydrous forsterite as a function of water content at different buffered conditions (MgO-buffered and SiO_2-buffered).
Forsterite aggregate with various water contents were synthesized at MgO- and SiO_2-buffered conditions from 4 GPa to 8 GPa, 1373 K in a multi-anvil apparatus. Water content was determined by FTIR using Paterson calibration and occasionally SIMS. Absorption peaks of FTIR were assigned to different sites and water contents in each specific site were calculated. Electrical conductivity measurements were performed at the same pressure from 500 to 800 K.
The maximum water content in MgO-buffered sample (1500 wt. ppm) at 4 GPa was found to be near 10 times that of SiO_2-buffered sample, indicating its superior water storage capacity. Compared with water content calibrated by Paterson method, SIMS measurement usually gives more than 3 times and more than 1.5 times amount of water for MgO-buffered sample and SiO_2-buffered sample respectively at 4 GPa. FTIR spectra in the former shows extremely high intensity of peaks at wavenumbers higher than 3500 cm^{-1} , while broad and noisy peaks at lower wavenumbers dominate in the latter. Peak assignment shows a dominance of hydrogen associated with silicon site in MgO-buffered sample and magnesium site in SiO_2 -buffered sample. With increasing pressure, difference in FTIR spectra in these two buffered conditions minimized. Both samples were dominated by peaks at wavenumbers higher than 3500 cm^{-1}, indicating an increasing preference of hydrogen for silicon site at 8 GPa even in SiO_2-buffered forsterite. Water content measured by SIMS in one SiO_2-buffered sample is more than 3 times that of FTIR calibration, similar to the situation of MgO-buffered at lower pressure.
For electrical conductivity measurement, high resistance of forsterite close to the background insulation at low temperature and dehydration at relatively higher temperature prohibited us to obtain good spectra. Preliminary results show that for MgO-buffered sample at 4 GPa, electrical conductivity increases with increasing water content (from 760 wt. ppm to 1470 wt. ppm) while their activation enthalpies decrease from 0.79 eV to 0.61 eV. For SiO_2-buffered sample, activation enthalpy is 1.23 eV for the only one sample. And its extrapolated conductivity to lower temperature crosses with that of MgO-buffered sample containing about 800 wt. ppm water at around 675 K. Combined with the FTIR peak assignment, such coincidence is probably caused by a different contributing factor of hydrogen in different sites. To verify our speculation, more experiments are needed, both at 4 GPa and 8 GPa. To prevent early dehydration during conductivity measurement, new setups aimed at controlling water fugacity will be tried.

Keywords: Proton conduction, Hydrous forsterite, Hydrogen position, Incorporation preference, Peak assignment and deconvolution

Occurrence of plate-like behavior and deep mantle water absorption in hydrous mantle convection system – 'Burst' of mantle water content

*Takashi Nakagawa[1], Hikaru Iwamori[2,3]

1. MAT, JAMSTEC, 2. D-SEG, JAMSTEC, 3. Department of Earth and Planetary Sciences, Tokyo Institute of Technology

We investigate the occurrence of plate-like behavior in hydrous mantle dynamics as a function of friction coefficient and its influence on evolution of the mantle water content. The hydrous mantle model can generate the long-term plate-like behavior with the higher friction coefficient, taken from Byerlee's law of brittle deformation, than the dry mantle, which is consistent with petrological estimate. The strength of oceanic lithosphere corresponding to friction coefficient plays a significant role with creating the global-scale mantle heterogeneity in hydrous mantle convection as well as strength of viscosity dependence due to water content. In vigorous plate motion, the mantle water content indicated rapid increase by up to 4–5 ocean masses called as the 'burst' effect. A 'burst' is related to the mantle temperature and water solubility of mantle transition zone. When the mantle cools below ~2380 K, mantle transition zone could store water transported by subducted slabs that can pass through the 'choke-point' of water solubility. The onset of 'burst' effect is strongly dependent on the friction coefficient, which gets delayed as the friction coefficient gets higher. The 'burst' effect of mantle water content could have seriously influenced the evolution of surface water ocean if the burst started early in which the Earth's surface cannot preserve the surface water ocean over the age of the Earth. This suggests that the boundary condition should be represented as a finite volume of surface ocean rather than constant water content of oceanic crust as a function of time (infinite water reservoir).

Keywords: water, mantle, plate motion

Reactions of chromite with olivine at high pressures with implications for ultrahigh pressure chromitites

*Masaki Akaogi[1], Airi Kawahara[1], Hiroshi Kojitani[1], Kazuaki Yoshida [1], Yuki Anegawa[1], Takayuki Ishii[1]

1. Department of Chemistry, Faculty of Science, Gakushuin University

Podiform chromitites which contain high-pressure minerals such as diamond and coesite as mineral inclusions are called ultra-high pressure (UHP) chromitites. The UHP chromitites were found in the Luobusa ophiolites of Tibet and Ray-Iz massif of the Polar Urals. Recently, mantle recycling models of the UHP chromitites have been proposed, in which the podiform chromitites were formed at shallow levels of the upper mantle, subducted into the transition zone, and returned to the earth's surface (Arai, 2013, Griffin et al., 2016). However, high-pressure experimental studies on chromitite would be insufficient to evaluate the mantle recycling models. Therefore, as a simple system for natural chromitites, we examined phase transitions in the system $MgCr_2O_4$-Mg_2SiO_4 at the conditions of the transition zone and the upper part of the lower mantle.
High-pressure high-temperature experiments were performed at 9.5-27 GPa at 1600 °C in $MgCr_2O_4Mg_2SiO_4$ composition with Kawai-type multianvil apparatus. The synthesized samples were examined by micro-focus and powder X-ray diffraction methods and by composition analysis using a scanning electron microscope with an energy-dispersive X-ray spectrometer.
The results indicate that complex, sequential phase changes occur in the system, as follows. Mg_2SiO_4 olivine (Ol) coexists with $MgCr_2O_4$-rich chromite (Ch) up to 13 GPa. However, above the pressure, they react to form garnet (Gt), $Mg_{14}Si_5O_{24}$-rich anhydrous phase B (Anh-B) and modified ludwigite (mLd) type $Mg_2Cr_2O_5$ phase. At 20 GPa, Anh-B was replaced with wadsleyite (Wd). At 21-23 GPa, $MgCr_2O_4$-rich calcium-titanate (CT) type phase coexists with ringwoodite (Rw). Above 23 GPa, $MgSiO_3$-rich perovskite (Pv, bridgmanite), periclase (Per) and CT are stable. In the transition sequences, the stability pressure of Anh-B is consistent with that in $Mg_{14}Si_5O_{24}$ in our recent study.
Based on the analyzed compositions of the coexisting phases, we calculated mineral proportions and densities of the above phase assemblages by mass balance calculation. Accompanying with the changes of phase assemblages, density increases from 3.84 g/cm^3 of Ol + Ch to 4.10 g/cm^3 of Gt + Anh-B + mLd, and finally to 4.43 g/cm^3 of Pv + Per + CT.
Our experimental results on the phase changes in the system are different from those postulated in the mantle recycling models of the UHP chromitites. In the models, it is assumed that no reactions occur between Ol and Ch and also transitions of Ol to Wd and of Ch to CT separately occur. Because evidences on the reaction products, Gt + Anh-B (or Wd) + mLd, have not yet been reported in the UHP chromitites, our experimental results suggest that the UHP chromitites did not experience P, T conditions of the transition zone and therefore recycled within the upper mantle. If the reaction products are found in the chromitites in future, they would be good indicators showing how deep the chromitites were subducted.

Keywords: ultrahigh pressure chromitite, chromite, mantle recycling, transition zone, high-pressure experiment

Thermodynamic calculations of high-pressure phase relations in the systems Mg_2SiO_4 and $MgSiO_3$

*Hiroshi Kojitani[1], Masaki Akaogi[1]

1. Department of Chemistry, Faculty of Science, Gakushuin University

Since Mg_2SiO_4 and $MgSiO_3$ are the most abundant endmembers of the Earth's mantle constituent minerals, their high-pressure phase relations have been investigated in detail by high-pressure high-temperature experiments. On the other hand, the stability of phases in the systems has been also studied by thermodynamic approach in conjunction with the high-pressure experiments. In the thermodynamic calculation of phase equilibrium boundary, thermodynamic parameters such as enthalpy, entropy, heat capacity, thermal expansivity and bulk modulus reported by different researchers are used. Some thermodynamic parameters which have not been experimentally obtained are optimized using experimentally determined phase boundaries. From these reasons, the thermodynamic parameters for one material are sometimes not internally consistent. This causes large uncertainties in the calculated phase equilibrium boundaries.

Recently, more accurate enthalpy, heat capacity and entropy data and equations of state for high-pressure polymorphs in Mg_2SiO_4 and $MgSiO_3$ and their constituent oxides have been experimentally determined. In this study, the internally consistency among the thermodynamic parameters for each material was examined. For example, high-temperature isobaric heat capacity of a high-pressure phase which collapsed by heating at 1 atm was estimated by the following method. Isochoric heat capacity was calculated using a vibrational density of state model which reproduced experimentally determined low-temperature heat capacity. The contribution of anharmonic effect was, then, added to the isochoric heat capacity using the same thermal expansivity and bulk modulus as those applied to the equation of state of the high-pressure phase. In addition, formation enthalpies for all the phases in the systems Mg_2SiO_4 and $MgSiO_3$ considered in the present calculations were determined from the difference in drop-solution enthalpy between constituent oxides and them. This gives unified relative enthalpy relations among the materials. Finally, using the obtained thermodynamic data set, we calculated high-pressure phase relations in the Mg_2SiO_4 and $MgSiO_3$ systems up to 26 GPa and 2300 K in dry condition.
In both the systems, calculated phase boundaries are consistent with those determined by high-pressure in situ experiments. It is noteworthy that, in the Mg_2SiO_4 system, the calculation result predicts the existence of the stability field of $MgSiO_3$ akimotoite + MgO between Mg_2SiO_4 ringwoodite and $MgSiO_3$ bridgmanite + MgO below about 1500 K. In subducted slabs whose temperature would be lower than that of surrounding mantle rocks, ringwoodite might first decompose to akimotoite + ferropericalse with increasing pressure and then transform to bridgmanite + ferropericlase.

Keywords: mantle minerals, Mg2SiO4, MgSiO3, thermodynamic stability, high-pressure phase relation

Fate of $MgSiO_3$ post-perovskite in super-Earths

*Koichiro Umemoto[1], Renata Wentzcovitch[2], Shunqing Wu[3], Kai-Ming Ho[3], Min Ji[3], Cai-Zhuang Wang[3]

1. Earth-Life Science Institute, Tokyo Institute of Technology, 2. Columbia Universitity, 3. Iowa State University

$MgSiO_3$ post-perovskite (ppv) is the final form of $MgSiO_3$ in the Earth. However, what happens in super-Earths in which pressure and temperature are much higher than those of the Earth's lower mantle? Understanding of fate of $MgSiO_3$ ppv under ultrahigh pressures is crucial for nature of interiors of super-Earths. Computational studies so far have predicted several pressure-induced dissociations of $MgSiO_3$ in super-Earths. Recent studies agree that $MgSiO_3$ ppv undergoes three-stage dissociations involving MgO, SiO_2, Mg_2SiO_4, and $MgSi_2O_5$ [1,2]. Based on these studies, we reinvestigate the high PT phase diagram of MgO-SiO2 system and we propose a new phase transition in MgO-SiO_2 system in super-Earths. Clapeyron slope of the new transition and thermodynamic quantities calculated for these phases should provide fundamental information for numerical simulation of mantle dynamics in super-Earths.

[1] S. Q. Wu, M. Ji, C. Z. Wang, M. C. Nguyen, X. Zhao, K. Umemoto, R. M. Wentzcovitch, K. M. Ho, J. Phys. Condensed Matter, **26**, 035402 (2014).
[2] H. Niu, A. R. Oganov, X. Q. Chen, and D. Li, Sci. Rep. **5**, 18347 (2015).

Keywords: MgSiO3 post-perovskite, pressure-induced phase transition, first-principles calculation, terrestrial exoplanets

High body wave attenuation in the upper mantle and the role of melt

*Geoffrey A Abers[1], Zachary C Eilon[2,3]

1. Cornell University, 2. Brown University, 3. University of California Santa Barbara

Seismic attenuation offers a powerful constraint on the physical state of the Earth’ s interior. Anelastic processes can generate strong variation in amplitudes and wave speeds of P and S waves, seen in both regional and teleseismic observations. The effect of temperature on attenuation in mantle rocks is reasonably well calibrated in the laboratory. However, these laboratory predictions deviate systematically from seismic observations. We demonstrate this with analysis of a new ocean-bottom seismometer dataset spanning the Juan de Fuca plate and ridge system, measuring seismic attenuation and velocity across an entire oceanic plate. Spectral ratios of teleseismic P and S waves show the highest attenuation anomalies and largest delays at in a narrow zone <50 km from the Juan de Fuca and Gorda ridge axes, with implied seismic quality factor for shear waves (Qs) 25 (extrapolated to 1 Hz) over the upper 150 km of the mantle beneath the ridge, among the lowest observed worldwide. We compare these results with measurements of Qs in subduction zones, observed from regional intraslab earthquakes. In those data, attenuation is strongest (Qs ~ 20-70) for paths traversing the mantle beneath arcs and backarcs. Although these two sets of observations (teleseismic Qs beneath a ridge and regional Qs beneath arcs) are made at different frequencies, when corrected for laboratory-calibrated frequency dependence they show comparable values. However, these Qs values are 2-5 times lower than predicted for any reasonable extrapolation of laboratory measurements in dry rocks. We infer a large effect of melt on Qs both beneath ridges and beneath arcs, with forward calculations suggesting up to 2% in situ melt.

Keywords: mid-ocean ridge, subduction zone, seismic attenuation

Viscosity of silicate melts at high pressure measured by *in-situ* falling sphere method

*Longjian Xie[1], Akira Yoneda[1], Daisuke Yamazaki[1], Yuji Higo[3], Denis Andrault[2], Geeth Manthilake[2], Boulard Eglantine[4], Guignot Nicolas[4]

1. Institute for Planetary Materials, Okayama University, 2. The Laboratoire Magmas et Volcans , 3. Japan Synchrotron Radiation Research Institute, 4. Synchrotron SOLEIL

The Earth experienced an early episode of magma ocean, in particular after the giant Moon-forming impact. Some partial melting still occurs today in the upper mantle. The viscosity of magma is a key to understand the various magmatic processes that can occur within the Earth. However, the accurate measurement of the silicate melt viscosity at high pressure has been limited to 13 GPa due to the high melting temperature and extremely low viscosity of silicate melt. We succeeded to extend the viscosity measurement to higher pressure by devising the *in-situ* falling sphere viscometry with boron doped diamond heater and ultra-fast cameral (1000 f/s) in Multi-anvil apparatus. Boron doped diamond is an ideal heater material for *in-situ* falling method because of its X-ray transparency and refractoriness exceeding 3000 C.
Viscosities of forsterite and diopside compositions were measured at 10 GPa, just above the liquidus temperature.The viscosity of enstatite composition was measured twice at 10 and 15 GPa, to confirm the good reproducibility.The viscosity of forsterite, enstatite, and diopside composition at 10 GPa are measured to be 0.023, 0.023 and 0.038 Pa.s, respectively. Forsterite and enstatite melts have similar viscosities, while diopside melt has much higher viscosity.The viscosity of forsterite composition at 15 GPa is 0.013 Pa.s, which is much lower than that at 10 GPa.
The experimental pressure range can be extended to higher than 23 GPa with the present cell assembly. The viscosity data at the higher pressure can be used to constrain the partitioning of gravity energy between the metal and silicate melts during the core formation. It can be used as well to estimate the largest grainsize of crystals entrained during the magma ocean solidification, which enables us to distinguish fractional or batch solidification of the magma ocean.

Keywords: viscosity, silicate melts, boron doped diamond, high pressure

Geo-neutrino measurement with KamLAND

*Hiroko Watanabe[1]

1. Research Center for Neutrino Science, Tohoku University

The **Kam**ioka **L**iquid-scintillator **A**nti-**N**eutrino **D**etector (KamLAND) is located in a rock cavern in the Kamioka mine, 1,000 m below the summit of Mt. Ikenoyama in Japan. KamLAND is marked by the ability to detect low-energy anti-neutrino signals at 1,000 tons of ultra pure liquid scintillator (LS) through the inverse β reaction. We demonstrated the oscillation nature of neutrino flavor transformation by observing electron anti-neutrino from nuclear reactors and neutrino properties have been explored precisely. Since neutrinos interact with other particles only via weal interaction, they have extremely low reaction probabilities. Such elusive property of neutrinos provides us with the ability to investigate optically invisible deep interior of the astronomical objects, such as the Earth. Neutrino measurement evolved understanding of neutrino properties to utilization of neutrino as a “probe”.
The detection of geo-neutrinos, anti-neutrinos produced in β-decays from primordial radioactivite elements (uranium, thorium and potassium) within the Earth’s interior, brings unique and direct information about the Earth’s interior and thermal dynamics. KamLAND detects geo-neutrino signals above 1.8 MeV due to the reaction threshold energy of the inverse β-decay, resulting to have sensitivity to anti-neutrinos from the decay chains of ^{238}U and ^{232}Th. The KamLAND collaboration reported the result of the first study of geo in 2005. Later the geo signals at KamLAND were used to estimate our planet’s radiogenic heat production and constrain composition models of the bulk silicate Earth (BSE). Following the Fukushima nuclear accident in March 2011, the entire Japanese nuclear reactor industry, which generates >97% of the reactor neutrino flux at KamLAND, has been subjected to a protracted shutdown. This unexpected situation allows us to improve the sensitivity for geo-neutrinos. In 2016, we presented that KamLAND started to have a sensitivity of Th/U mass ratio of entire Earth.
Currently, geo-neutrino observed rate is in agreement with the prediction from existing BSE composition models within 2 σ C.L., but some extreme models start to be disfavored. This ability to discriminate is limited by the experimental uncertainty and crust modeling. Continuing the data taking under the present low-reactor situation yields better signal-noise ratio and provides promising power of uncertainty. Enhanced geo-neutrino flux calculation model using latest crustal structure model and geochemical understanding around Japan Island Arc will be a key issue for the further constraint on the Earth models and observation of mantle contribution.

Keywords: Geo-neutrino, radiogenic hear, Th/U mass ratio

Defining the deep Earth with the OBK detector

*William F McDonough[1]

1. RCNS & Earth Sciences, Tohoku University, Sendai, Japan

The global surface heat flow reflects the combine contributions of primordial and radiogenic heat, with the former comprised of accretion and core formation sources. The continental crust contributes 7 TW of radiogenic power and a sub-MOHO flux of 10 to 30 mW/m^2 for a total surface flux of 65 mW/m^2. The continents contribute about 1/3 of the total power lost from the Earth. At its present spreading rate, the oceans contribute 2/3 of this flux, but we do not know how much of this flux is primordial versus radiogenic contributions. Earth models collectively allow up to a factor of 30 in the spread of estimates of the present-day mantle’s radiogenic power. Moreover, the surface heat flux is likely to be a relative constant over the continents, whereas in the oceans it is unlikely to remain a constant over the last few billion years given variations in spreading rates. Our understanding of the Earth’s thermal evolution history is intimately linked to knowing the total radiogenic power of the mantle.

OBK (Ocean Bottom KamLAND) is the next generation underwater geoneutrino detector designed to measure the Earth’s abundance and distribution of Th and U inside the mantle. We have shown that such a detector is capable of identifying and mapping out large deep Earth structures (e.g., LLSVP), where they have enrichments in these elements relative to the ambient mantle.

Following on from the successes of the existing detectors in Japan and Italy, we propose an international effort, with Japanese geoscientists and particle physicists leading, to construct and deploy an ocean-going detector (OBK) to (1) map out structures in the mantle, (2) constraint the cooling history of the planet, (3) distinguish continental and mantle Th/U ratios, which documents the Earth’s biological imprint on the mantle, and (4) define the power driving plate tectonics. Beyond these goals in Earth Sciences, this instrument will have spinoffs for particle physics and astroparticle physics. This field of science has been richly acknowledged by Nobel prizes; the science proposed here has the potential to continue this great tradition.

Keywords: geoneutrino, mantle, heat flow, radiogenic power, thermal evolution

Asteroid impact-induced magmatism and tectonics on the Hadean-Archean Earth

*Hiroshi Ohmoto[1], Uschi M. Graham[2]

1. The Pennsylvania State University, 2. Univ. of Kentucky

In the previous talk by Graham et al., we suggested that: (1) The numerous fragments of Ti-Fe-rich meteorites, discovered in the ~3.45 Ga Apex Basalt near Marble Bar, Western Australia, most likely represent parts of a large (~10-20 km diameter?) asteroid body that created a large (~150 km diameter?) impact-crater on a deep (2,000 m) ocean floor; and (2) The Apex Basalt (~3-4 km thick) represents the crater-fill basalt magmas that were generated by the impact-induced, rapid decompression-melting of the deep-mantle peridotite. The close similarities in the abundance ratios of the high-field-strength elements (e.g., REEs, Nb, Y, Zr) between the Apex Basalt and the 120-90 Ma Ontong Java Oceanic Plateau Basalt, which has been suggested by some researchers to be the product of an ~20-30 km-diameter bolide impact, support the above model for the magmatism in the East Pilbara district ~3.5 Ga ago.

We have extended the examinations of the geological, petrological, and geochemical characteristics of the pre-3.0 Ga geologic formations in the Pilbara- and Kaapvaal Cratons, and suggest the following models for the magmatism, tectonics, and evolution of the oceanic and continental crusts of the early Earth: (1) The Last Heavy Bombardment of asteroids lasted until at least ~3.2 Ga ago, possibly until ~2.5 Ga ago. (2) Prior to ~3.2 Ga (or ~2.5 Ga), magmatism and tectonics on the Earth were mostly dictated by the impacts of asteroids (mostly in the oceans), rather than by the plate (horizontal) tectonics or the plume (vertical) tectonics that are caused by the large-scale convections in the mantle. Punctuations of the thick oceanic (and continental) crusts, as well as the large-scale melt-generation in the upper mantle by large bolide-impacts provided the effective mechanism to release the interior heat of the early hot Earth. (3) Rapidly declining meteorite impact events after ~3.2 Ga (or ~2.5 Ga) was the probable cause for the initiation of the plate- and plume tectonics, because the Earth had to find alternative ways to release its interior heat. (4) All major igneous-rock formations in the Archean greenstone belts, including komatiite, basalt, and granitoiods, were formed from the magmas generated by impact-induced, rapid decompression-melting of mantle peridotite, and by the interactions between these magmas and the oceanic crust. (5) Until ~3.2 Ga (or ~2.5 Ga) ago, no significant difference in composition and thickness existed between the continental and oceanic crusts, i.e., the true continental crust did not exist. The oceanic (and continental) crusts were comprised of large circular/oval-shaped “blocks” (~10^6–10^7 km^2 in area) which were created by different asteroid impacts. Each “block” was chemically heterogeneous, and vertically zoned (generally by composition) from ultramafic in the lower zones to felsic in the upper zones. (6) The plate tectonics, which began ~3.2 Ga (or ~2.5 Ga) ago, caused preferential melting of the felsic to intermediate rocks (compared to the mafic and ultramafic rocks) of the Archean oceanic crust during its subduction, because of their lower temperatures of melting. The andesitic/felsic melts generated from the subduction zones ascended to create the continental crust. Because silicic continental crust is buoyant compared to the mafic oceanic crust, the continental crust has remained at a higher level than the oceanic crust since ~3.2 Ga (or ~2.5 Ga) ago. (7) Slower melting of the upper mantle peridotite by the hotter materials from the lower mantle in the post-Archean eras, compared to the rapid melting of the mantle peridotite due to sudden decompression caused by meteorite impacts during the Archean era, have created chemically homogeneous basalt magmas that have erupted at mid ocean ridges to create chemically homogeneous oceanic crust since ~3.0 Ga ago.

Keywords: Asteroid, magmatism, tectonics, early Earth

~3.45 Ga meteorite fragments suggest the Earth is poorer in Fe and Ni and richer in Ti and V than the current model

Uschi M. Graham[1], Zi-Kui Liu[2], *Hiroshi Ohmoto[2]

1. Univ. of Kentucky, 2. The Pennsylvania State University

Previous researchers have estimated elemental abundances of the solar system and of the Earth mostly from the compositions of carbonaceous chondrites and other meteorites that have fallen recently on the Earth. The modern metal-rich meteorites are comprised of Fe-Ni alloys (Ni contents 5-20 wt%) with minor Co.

In the ABDP #1 drill core from Marble Bar, Western Australia, we have discovered numerous fragments (up to ~2 mm in size and often >5 volume % of the rock) of metal-rich meteorites throughout a ~40 m section of the ~3.45 Ga Apex Basalt that overlies the thick (up to ~200 m) Marble Bar Cher/Jasper (MBC) beds. The meteorite fragments occur together with impact spherules made of the melted volcanic rocks, angular fragments of the MBC, and the tsunami-disturbed MBC beds. The underlying MBC beds exhibit shocked- and brecciated textures and host numerous quartz veinlets that intruded along the impact-induced fractures. These features, and the areal extents of the Apex Basalt (~3-4 km thick), suggest that the meteorite fragments are part of a large (~10-20 km diameter?) bolide that created a large (~150 km diameter?) impact crater on a deep (>2,000m) ocean floor, and that the Apex Basalt was the crater-fill basalt magma that was generated by the impact-induced, rapid decompression-melting of the mantle peridotite.

To our surprise, the meteorite fragments in the Apex Basalt have entirely different chemistries than the modern iron meteorites. They are mostly made of oxidized forms of Ti-Fe (Ti Fe) alloys with various amounts of Si, Al, V, Cr, and Cu as solid solutions; but Ni is very low (<0.1 wt%). Oxidation of the metal alloys probably occurred through reactions with the atmospheric O_2 in the “impact clouds”. Thermodynamic data suggest that the original metal-alloys in our meteorites were formed in the core of a planet with more reducing conditions than the cores of the planets that formed the modern iron meteorites. Our findings suggest that: (1) The asteroids that formed the early Earth may have had very different compositions than the meteorites that have fallen recently on the Earth--consequently, the early-Earth materials may have come from different parts of the asteroid belt than the modern meteorites; (2) The age of the Earth may be older (or younger) than 4.54 Ga, an age which was determined using the modern meteorites; (3) Elemental abundances of the solar system and of the Earth are possibly much higher in Ti and V, and lower in Fe and Ni, than those estimated by previous researchers. This would explain why the previously-estimated solar abundances for Ti and V are much lower (whereas those for Fe and Ni are much higher) than those estimated using the Oddo Harkin’s Rule of nucleosynthesis; and (4) The Earth’s core is possibly made of Ti-Fe-Si-Al alloys, rather than of Fe-Ni alloys. This would explain why the density of the core is much lighter than the densities of Fe-Ni alloys. It would also explain why the Moon, which formed at ~4.40 Ga, is characterized by Ti-rich basalts.

Keywords: Ti-rich meteorites, solar abundances, Earth's core

Compositional layering within the Large Low Shear-wave Velocity Provinces in the lower mantle

*Maxim Ballmer[1,2], Lina Schumacher[3], Vedran Lekic[4], Christine Thomas[3], Garrett Ito[5]

1. Institut für Geophysik, Departement für Erdwissenschaften, ETH Zürich, 8092 Zürich, Switzerland, 2. Earth-Life Science Institute, Tokyo Institute of Technology, Meguro, Tokyo 152-8551, Japan, 3. Institut für Geophysik, Westfä lische Wilhelms Universität Münster, 48149 Münster, Germany, 4. Department of Geology, University of Maryland, College Park, MD 20742, USA, 5. School of Ocean and Earth Sciences and Technology, University of Hawai‘i at Manoa, Honolulu, HI 96822, USA

The large low shear-wave velocity provinces (LLSVP) are thermochemical anomalies in the deep Earth’s mantle, thousands of km wide and ~1,800 km high. This study explores the hypothesis that the LLSVPs are compositionally subdivided into two domains: a primordial bottom domain near the core-mantle boundary and a basaltic shallow domain extending from 1,100~2,300 km depth. This hypothesis reconciles published observations in that it predicts that the two domains have different physical properties (bulk-sound vs. shear-wave speed vs. density anomalies), the transition in seismic velocities separating them is abrupt, and both domains remain seismically distinct from the ambient mantle. We here report underside reflections from the top of the LLSVP shallow domain, supporting a compositional origin. By exploring a suite of two-dimensional geodynamic models, we constrain the conditions under which well-separated “double-layered” piles with realistic geometry can persist for billions of years. Results show that long-term separation requires density differences of ~100 kg/m^3 between LLSVP materials, providing a constraint for origin and composition. The models further predict short-lived “secondary” plumelets to rise from LLSVP roofs and to entrain basaltic material that has evolved in the lower mantle. Long-lived, vigorous “primary” plumes instead rise from LLSVP margins and entrain a mix of materials, including small fractions of primordial material. These predictions are consistent with the locations of hotspots relative to LLSVPs, and address the geochemical and geochronological record of (oceanic) hotspot volcanism. The study of large-scale heterogeneity within LLSVPs has important implications for our understanding of the evolution and composition of the mantle.

Keywords: Mantle Convection, Primordial Reservoir

Origin of Seafloor, Platetectonics, Pacific arc basin, Proof of eccentric Moment Force, Mechanism of Plate rapid change of direction,

Verification by Abduction of "Multi Impact Hypothesis" explaining everything uniformly.

*Akira Taneko[1]

1. SEED SCIENCE Lab.

Structure and Dynamics of Earth and Planetary

Mantles Continental movement theory, Ocean Floor expansion theory, Driving force from Plate Tectonics to Plume Hypothesis was Thermal Convection Hypothesis.

We propose Celebrity Hypothesis that Minimizes Moment of Inertia caused by crushing crust Mantle defect and isostatic uplift eccentricity due to Inertial efficiency imbalance as **Plate new Driving Force**.

A Wegenr tried to prove **Continental drifft hypothesis** and prove it based on Continuity of paleontology and geology because Coastal profile of Africa coincides with that of continental North and South America.

Plate tectonics is now almost a fixed theory with empirical observations such as **Ocean Foor Epansion Hypothesis**, **Mantle Thermal Convection Hypothesis,** discovery of Atlantic mid-ocean ridge, discovery of transform faults, reversal of geomagnetism and submarine tape recorder Hypothesis.

However, **Driving force of Continental movement** *that Wegener could not show is* ***still a mystery*** *in* ***Plate Tectonics****.*

Wegener pointed out Effort to explore Origin of Deep ocean floor (-5 km) occupying 70%, Origin of Plate boundary, Origin of plate tectonics.

Arcuate archipelago and Origin of Basin still remain a mystery. A new paradigm capable of unifying all of this was desired.

It is Multi Impact Hypothesis by Abduction and was stated in "Elucidation of Missing link of Earth and Moon" from geophysics and solar system planetary theory.

According to it, in addition to Origins of this Plate Tectonics, Origin of Moon, Origin of Deep ocean floor, Core eccentricity, Origin of Jupiter's Great Red Spot, Origins of Mercury and Pluto, Origin of Asteroid belt and Differentiated Meteorite. It is a proposal of a new paradigm that can unravel Origin of Word.

Furthermore, I could also show Reason for Eccentric Density difference where Moon and Moon's Orbital Energy (theoretically calculated from Collision Energy) and Mantle matter are oriented on Same side.

Abduction is Idea that Correctness of Hypothesis is guaranteed to Extent that Conclusion by a certain Hypothesis can explain Current situation.

It is a big change of thinking and it is called creative reasoning,Abduction.

Using Physically Meaningful Hypothesis, if Idea is correct, a breakthrough progress is obtained.

"Multi Impact Hypothesis":About 4 billion years ago from the birth of the solar system, when CERRA orbital deformed due to Jupiter perturbation and ruptured by the tension of Jupiter and the sun, CERRA and the Earth were differentiated and solidified.

About 4 billion years ago from Birth of Solar system, when CERRA orbital deformed due to Jupiter's perturbation and ruptured by the tension of Jupiter and the sun, CERRA and Earth were differentiated and

solidified.
When Darwin's rise (convex plate) occurred in Collision Mantle Defect due to isostasy, Plate from which Surrounding crust had peeled recessed and Boundary Crack formed Arcuated Islands, Pacific Rim Arc Island concave arc.
Arcuate archipelago centered on Pacific Ocean and Java Island during Formation of Tacos Sea, a trench arc continuing to Outer side of Arcuate Island indicates that Convex Plate has slipped under Arcuate archipelago concave basin (= Mutual slipping mechanism of Plate).
Plate boundary is caused by cracks when multiple mantle fragments crash into Earth.

Proof of inertial efficiency eccentric moment driving force
In this Hypothesis, since Earth rotates on its own axis, in Earth where Moment of Inertia becomes uneven (unbalanced) when Missing mantle is isostasic due to collision, Driving force that minimizes Moment of Inertia is generated.
Reason for sudden change in movement direction and Mechanism of rotation axis Inclination
Impact fracture at single mantle collision works on Opposite side of Earth as Ejection pressure from Inside.
Formation mechanism of Diamond mine is indicated by Formation of a kimber-lite pipe.
Collision with Drake Passage is Cause of Diamond mine in Russia Miruuui.
A tilt of 23.5 ˚was formed on Axis of rotation from the revolving surface due to the couple of collision to high latitude.
There are three rows of curved trajectories parallel to plate movement traces of Hawaiian Islands and Kuril Seamount line
It is a result in Direction of plate movement, which is caused by a sudden change in Rotation Axis.

- Evolution of Earth only once -Demonstrated by history -
Ability to explain all Mysteries as a unified Evolution alone with one Hypothesis is verification by Abduction of "Multi Impact Hypothesis".
It is expected that quantitative simulation becomes possible in more detail from Qualitative Elucidation.

Keywords: Origin of Ocean floor, Origin of the "Moon formation and the Earth's plate tectonics", Proof of inertial efficiency eccentric moment driving force, Origin of the Pacific Rim Arc Isolated Archipelago Back Arc Basin, Mechanism of Slipping Inside Plates, Plate movement direction rapid change mechanism reason, Verification by abduction - by one-time evolution of the earth and empirical history -

Origin of the Earth,Plate-tectonics,Ocean-floor, by Abduction in Multi-Impact Hypothesis CERRA

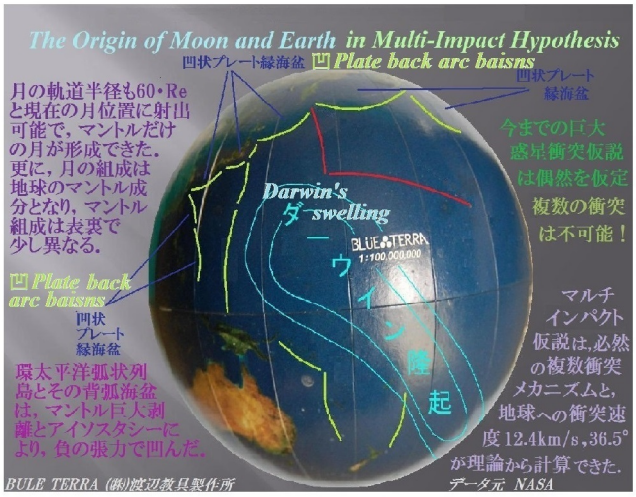

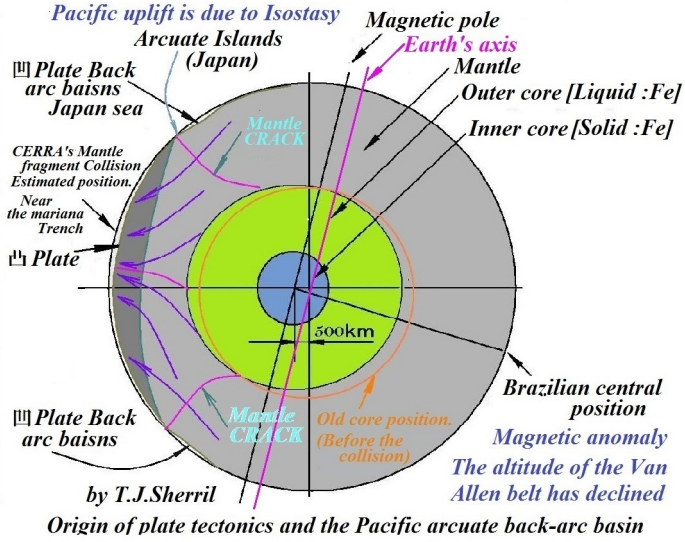

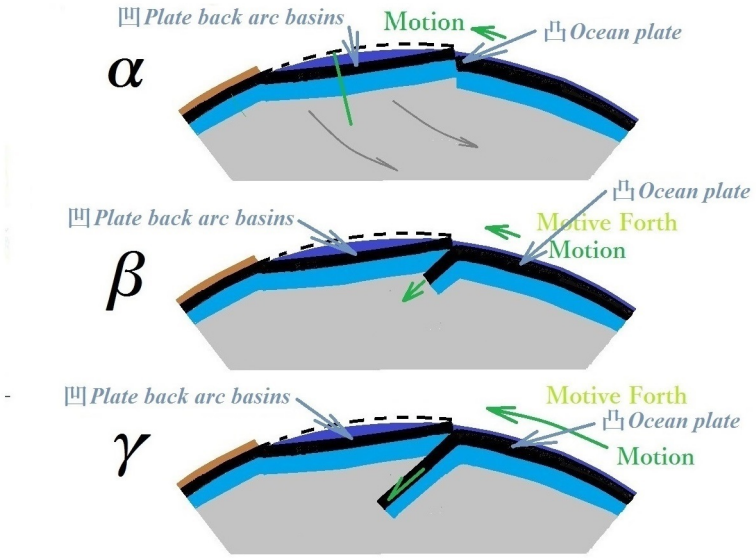

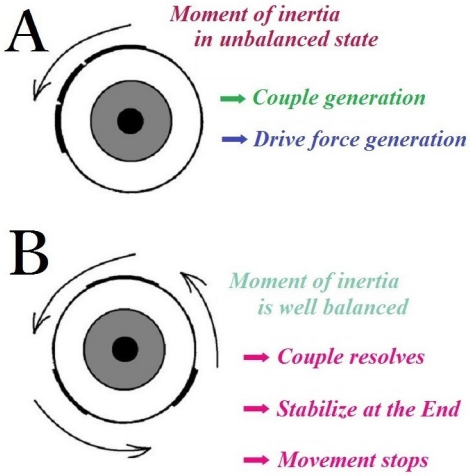

Phase Transformation Mechanism Responsible for Deep-focus Earthquakes by The Multi-Phase-Field Methods

*Sando Sawa[1], Masanori Kido[1], Rei Shiraishi[1], Jun Muto[1], Hiroyuki Nagahama[1]

1. Department of Earth Science, Tohoku University

One of the possible mechanisms for deep-focus earthquakes is the faulting associated with phase transformation from olivine to spinel under high pressure. Burnley et al. (1991) conducted deformation experiments of Mg_2GeO_4 under conditions at confining pressures of 1~2 GPa, temperature of 900~1500 K and strain rates of 2×10^{-5} ~ 2×10^{-3} s^{-1}. The spinel is observed like microscopic lenses in place of microcracks. They form perpendicular to the maximum compressive direction, which is called "anticracks." They connect with each other, eventually, cause the faulting. Spinel anticracks can be formed by intracrystalline nucleation and nucleation at grain boundaries. As the mechanism, it has been advocated that they form by nucleation whose crystal orientation is random, martensitic transformation or along the dislocation. However, we don't know which is a dominant mechanism forming spinel anticrack. So, to reveal how spinel anticracks are formed, we have studied the transformation mechanics by the Multi-Phase-Field (MPF) method. The MPF method is a phenomenological model based on continuum mechanics and has widely used in material sciences. We can reveal temporal change of material morphology by MPF method, that is, easily follow crystal interfaces with probability. We developed the numerical model taking into account of both intracrystalline nucleation and nucleation at grain boundaries. Furthermore, to constrain physical conditions of the numerical model, we also conducted experiments by a Griggs type piston-cylinder apparatus using solid NaCl as a confining medium based on Burnley et al. (1991) to observe microstructure of a deformed sample. We compressed Mg_2GeO_4 as an analogue material under conditions at confining pressure of 1.2 GPa, temperature of 1200 K and strain rate of 2.0×10^{-4} $s^{-1}$where Burnley et al. (1991) reported faulting by anticrack mechanism. As a result of the experiment, the sample was ductile deformed. According to the microstructural observation on the deformed sample, there are many bands composed of very-fine grained materials. The particle size is very small and there are small faults in the vicinity, so we think that superplastic deformation in these fine-grained portions might cause faulting, as proposed by Burnley et al. (1991). Also, compared to hydrostatic experiment in which fine grain materials were observed but phase transformation didn't occur, we inferred that phase transformation is difficult to occur without differential stress. Therefore, we modified the conditions of numerical model to consider superplastic deformation and particle size, finally, built up new numerical model.

Keywords: Deep-focus earthquakes, Phase Field, Griggs type piston-cylinder apparatus

Stability of anhydrous phase B, $Mg_{14}Si_5O_{24}$, at the mantle transition zone conditions

*Liang Yuan[1,2], Eiji Ohtani[1], Akio Suzuki[1], Zhenmin Jin[2]

1. Department of Earth and Planetary Materials Science, Tohoku University, 2. School of Earth Sciences, China University of Geosciences (Wuhan)

Stability of anhydrous phase B, $Mg_{14}Si_5O_{24}$, has been determined in the pressure range of 14-21 GPa and in the temperature range of 1100-1700˚C with both normal and reverse experiments at high pressures and high temperatures. Our results imply that anhydrous phase B is stable at the *P-T* conditions corresponding to the shallow depth of the mantle transition zone and it decomposes into periclase and wadsleyite at greater depth. The decomposition boundary of anhydrous phase B into wadsleyite and periclase has a positive phase transition slope and can be expressed by the following equation, P(GPa)= 7.5 + 6.6 x 10^{-3}T(˚C). Configuration disorder might account for an increase of entropy for anhydrous phase B at high-temperature conditions. It is suggested that MgO-rich conditions can be available in the deep mantle during hydrous melting of peridotite and the reduction of subduction carbonates by the metal-saturated mantle at depth > 250 km. Anhydrous phase B might become an important phase in the area where SiO_2 activity is low. We propose that the paragenesis of directly touched ferropericlase-olivine inclusions in natural diamonds might be the retrogression products of anhydrous phase B via the decomposition reaction Anh-B = Olivine + Periclase during the transportation of host diamonds from the deep to the surface. Our experimental results put a constraint on the origin of such diamonds at a depth less than 500 km. On the cooling of the magma ocean during the early history of the Earth, a distinctive layer that was concentrated with hydrogen and other elements such as Fe, Ca, Mn substituting Mg might exist with the crystallization and accumulation of anhydrous phase B at depth equivalent to the upper part of the mantle transition zone.

Keywords: Anhydrous phase B, phase relations, Clapeyron slope, diamond inclusions, Raman spectra

Numerical simulations on the formation and behaviors of slabs in 2-D spherical annulus

*Mana Tsuchida[1], Masanori Kameyama[1]

1. Geodynamics Research Center, Ehime University

We developed a numerical model of thermal convection of highly viscous fluid in a two-dimensional spherical annulus, aiming at (i) classifying the morphologies and dynamic behaviors of subducting slabs, (ii) comparing the shapes of slabs obtained in our simulation models with those estimated from seismic tomography to offer the constraints on the plate velocities and the properties of the 660 km discontinuity from fluid-dynamical viewpoints.
In this study, we consider a time-dependent convection of fluid under the extended Boussinesq approximation. The viscosity of mantle material is assumed to be exponentially dependent on temperature and pressure (or depth). We also have included the exothermic olivine to spinel phase transition at around 410 km depth and the endothermic post-spinel phase change at around 660 km depth. The plate subduction is modeled by downward flow of cold and viscous fluid along with a conduit which guides the descending slab from surface to the mantle transition zone. We take into account the effect of trench migration, by imposing the migration of the conduit with respect to the deep mantle.
We found that our model successfully reproduces the diverse morphology of subducting slabs which can be well compared with those of natural slabs, by carrying out calculations with systematically varying the velocities of subducting slabs and trench migration, the Clapeyron slope at around 660 km depth, and the viscosity jump between the upper and lower mantle. In particular, the dynamic behaviors of slabs around the mantle transition zone can be classified into five types depending on the combinations of varying parameters: (1) Penetrating, (2) Accumulating, (3) Floating, (4) Long-term Stagnation, and (5) Short-term Stagnation.
A careful comparison of the slab morphologies in our numerical experiments with those of natural slabs in selected subduction zones enabled us to estimate the rate of trench migration with respect to the deep mantle, given that both the duration of subduction and rate of two-plate convergence are properly known. This implies that the morphology of slabs can be used to settle a reference frame of motions of surface plates, which is of crucial importance in determining their absolute velocities from the relative ones. Such comparison could also offer fluid-dynamical constraint on the properties of the 660 km discontinuity.

Keywords: subducted slab, stagnant slab, mantle convection, numerical simulation

Fabrication of highly-dense and fine-grained olivine aggregates with various crystallographic preferred orientation patterns in natural peridotite rocks

*Sanae Koizumi[1], Thoru S Suzuki[2], Yoshio Sakka[2], Kosuke Yabe[1], Takehiko Hiraga[1]

1. Earthquake Research Institute,The University of Tokyo, 2. National Institute for Materials Science

Olivine is the most abundant mineral in the Earth’ s upper mantle and it is considered to orient crystallographically in response to the mantle flow. Six types of fabrics have been identified in mantle peridotite: A, B, C, D, E and AG type. Physical properties of olivine such as elasticity, plasticity, thermal conductivity, thermal expansion and electron conductivity are known to be anisotropic so that geophysical observations showing directional dependence in the mantle are often attributed to the result of crystallographic preferred orientation (CPO) of the mineral. However, most of our current understanding of the effects of CPO on physical properties of bulk rocks is essentially based on the properties of single crystals.
To measure CPO effect on the bulk rock properties directly by room experiments, it is required to prepare polycrystalline materials with ideally controlled CPO
Olivine particles synthesized from source oxide powders and natural mineral particles prepared from milling natural olivine crystals were used in this study. To fabricate olivine aggregates with CPO, an external strong magnetic field (12 T) was applied to the olivine fine particles which were dispersed in the solvent. The alignment of certain crystallographic axes of the particles with respect to the magnetic direction was anticipated due to magnetic anisotropy of olivine. The dispersed particles were gradually consolidated on a porous alumina mold, which was covered with a solid-liquid separation filter, during drainage of the solvent. The consolidated aggregate was then isostatically pressed and vacuum sintered.
Uni-axially aligned *c*-axes and *b*-axes olivine aggregates that correspond BC-type and AC-type peridotite were obtained from the aggregates aligned under static and rotated magnetic field, respectively.
Tri-axially aligned olivine aggregates corresponding to A-, B-, C- and E-type peridotite were obtained from a modulated rotation magnetic field.

Keywords: crystallographic preferred orientation, olivine, mineral aggregate

High-resolution 3-D S-wave structure beneath North America using phase and amplitude of surface waves

Kouta Hamada[1], *Kazunori Yoshizawa[1,2]

1. Graduate School of Science, Hokkaido University, 2. Faculty of Science, Hokkaido University

Majority of surface wave tomography have employed the phase information, which reflects the average phase speed perturbation along a propagation path. To the contrary, the use of amplitude anomalies of surface waves has been limited in tomographic studies, due to a variety of uncertain factors such as source mechanism, local amplification at receiver, elastic focusing/defocusing and anelastic attenuation. In the interstation analysis, the source term can be canceled out, so that we can focus on the effects of the elastic focusing/defocusing as well as the receiver amplification factors, with an appropriate correction for anelastic attenuation. In the framework of ray theory, the amplitude anomalies affected by the focusing/defocusing reflect the second derivatives of phase speed across the ray path, and thus the amplitude data are more sensitive to shorter-wavelength structure than the conventional phase data.

In this study, we employ a fully non-linear waveform fitting technique to measure interstation phase speeds and amplitude ratios simultaneously, based on a global optimization method. This technique is applied to observed seismograms of the high-density transportable array deployed in the United States (USArray) in the past decade, and a large-number of interstation phase speed and amplitude ratio data are collected. The typical interstation distances for measured dispersion data are less than 1000 km, which is much shorter than the average path length used in conventional single-station analysis and can be of help in improving the lateral resolution of the regional tomography models.

The measured interstation phase and amplitude data are inverted simultaneously for phase speed maps as well as local amplification factor at each receiver location. The phase speed maps derived from both phase and amplitude measurements exhibit better recovery of the strength of velocity perturbations, particularly for the smaller-scale heterogeneities. The spatial distributions of local amplification factors in the longer period are correlated well with the velocity structure in the upper mantle, indicating that the effects of local amplification can be isolated well from those of focusing in our joint inversion of phase and amplitude data.

Isotropic and anisotropic 3-D S wave speed models of North American continent are then obtained from the phase speed maps. Our isotropic 3-D S wave models from phase and amplitude data for Rayleigh waves emphasize local-scale tectonic features associated with conspicuous lateral velocity gradients; e.g., fast anomaly in the Colorado Plateau surrounded by slow anomalies, and slow anomaly in the New Madrid Seismic Zone encompassed by faster regions. Such local tectonic features with the size of about 200 km can hardly be identified in the conventional surface wave tomography, and thus the interstation amplitude ratio data can be of great help in improving the lateral resolution of velocity models in the upper mantle. Radial anisotropy models derived from the phase speed maps of Rayleigh and Love waves using only phase data, are also constructed. The results show faster SH wave speed anomaly than SV in the tectonically active regions in the western and central U.S., while the model exhibits faster SV wave speed anomaly than SH in the eastern region below 75 km depth.

Keywords: upper mantle, surface wave amplitude, North American Continent

Dvelopment of S wave buffer rod for DAC-GHz experiments.

*Akira Yoneda[1]

1. Institute for Study of the Earth's Interior, Okayama University

I have been develping GHz ultrasonic technique for diamond anvil cell (DAC) in a recent a few years. Last year, I reported the development of P wave GHz buffer rod. Then, I conducted development of GHz S wave buffer rod as well. Simultaneopusly, I have examined how to get a good signal through P wave buffer rod. The solution is combination wiping by aceton, alcohole, and ammonia water. I have started the measurement for the specimen squeezed in DAC. In the poster, I will show those effort.

Keywords: GHz ultrasonics, diamond anvil cell, Shera wave, mantle, elasticity, high pressure

P and SH wave upper mantle velocity structure beneath South China

*yi sui[1], rui qing zhang[1], qing ju wu[1]

1. Institute of Geophysics China Earthquake Administration

There is widespread intracontinental orogen and magmatic province in Mesozoic South China. Study of upper mantle velocity can bring light on the distribution and movement of material in deep earth of this region. Triplication waveform of P and SH from 5 to 30 degree recorded by CDSN(Chinese Digital Seismic Network) are used to obtain P and SH wave upper mantle velocity structure by comparing with synthetic waveform. There is low velocity layer above 410 in both P and S waveform, and 410km discontinuity is broadened. Low P and low S velocity and high Vp/Vs may be result of partial melting related to plate subduction.

Keywords: triplciation, upper mantle , partial melting

Tidal Dissipation of the Solid Earth with an Internal Structure Including a Low-Viscosity Layer

*Yuji Harada[1], Koji Matsumoto[2]

1. Lunar and Planetary Science Laboratory, Space Science Institute, Macau University of Science and Technology, 2. RISE Project Office, National Astronomical Observatory of Japan, National Institutes of Natural Sciences

Tidal dissipation in the solid Earth is one of the important geophysical phenomena. Because tidal dissipation in a solid body depends on its internal structure, especially its viscosity structure, the dissipation can be a constraint on the interior. If the viscous structure can be constrained, it may provide one of the useful clues to learn the mantle dynamics.

The tidal response of the solid Earth, particularly the dependence of the theoretical Love number on the tidal period and viscosity structure, has been investigated in a few previous studies already. As a result, it has been considered that the presence of a low-viscosity layer inside the mantle, especially at its bottom part, is important for successfully interpreting the frequency-dependence of the observational Love number derived geodetically.

On the other hand, based on a similar idea to that of the above-mentioned research, the authors examined the dependence of the tidal quality factor on the frequency and the internal structure, assuming that such a low-viscosity layer exists also in the mantle of the Moon. This result also indicates that, as well as the Earth, the frequency-dependence of the quality factor obtained from the selenodetic observation can be explained if a low-viscosity layer exists at the base of the mantle. In addition, the characteristic timescale corresponding to the viscoelastic property of this layer is discovered to be very close to the main tidal periods. That is, it also implies a possibility that the viscosity which leads to efficient tidal heating in the layer is controlled through self-regulation.

Returning the viewpoint to the Earth tide with considering the implication from the lunar tide, it is unknown whether the above low-viscosity layer of the Earth possesses viscosity which is consistent with the dominant tidal periods. The previous research on the Earth have mainly illustrated the frequency-dependence of the complex Love number. Indeed, the uncertainty of the viscosity of the layer was systematically taken into consideration also in the previous analysis. However, the viscosity structure dependence of the quality factor obtained from the complex Love number was not explicitly specified. It is meaningful to survey this point in terms of both geophysics and comparative planetology.

Therefore, in the present study, in order to quantitatively estimate the effect of the low-viscosity zone at the bottom of the mantle on the tidal dissipation of the solid Earth, especially on the quality factor, the viscoelastic tidal deformation was calculated for several actual tidal periods. The typical reference structure for the density and elastic profiles is given in here based on the observation of seismic observation. Also, concerning the viscosity profile, for the sake of simplicity in order to roughly understand the dependence on the layered structure, just the four layers of a lithosphere, asthenosphere, mesosphere, and low-viscosity layer are set from the top to the bottom. Among them, only the viscosity of the low-viscosity layer is adjusted whereas those of the remaining three layers are uniform and constant. In the computation of the complex Love number in finding the quality factor, the stress-strain relation follows the rheological law of the Maxwell material. Then, the viscosity of the layer was estimated by comparing this theoretical value of the quality factor with the observational value.

The calculation result demonstrate that, like the Moon, the relaxation time of the low-viscosity layer is close to the tidal periods with respect to the deformation of the Earth. It is basically the same as the previous result that the numerical value matches with the geodetic observation if adding the influence of the low-viscosity layer. What is further clarified in this work is that the Maxwell relaxation time of the viscosity satisfying the frequency-dependent quality factor for the semidiurnal and diurnal tides, which is particularly prominent at the Earth tide, approaches the tidal period. In other words, a similar implication to that of the Moon described above were obtained here also in the case of the Earth.

Acknowledgments: This work was achieved using the grant of Research Funding 039/2013/A2 and 007/2016/A1 supported by the Science and Technology Development Fund of the Macau Special Administrative Region.

Keywords: Tidal Dissipation, Solid Earth, Internal Structure, Low-Viscosity Layer

Upper mantle structure beneath the Ontong Java Plateau from measurements of body wave differential travel times

*Takumi Kobayashi[1], Daisuke Suetsugu[2], Masayuki Obayashi[2], Hiroko Sugioka[1]

1. KOBE University, 2. Japan Agency for Marine-Earth Science and Technology

The Ontong Java Plateau(OJP) is a single largest oceanic plateau in the world, and thought to emplaced at 120Ma. To reveal the origin of the OJP, we have to know the structure beneath the OJP. Richardson et al. (2000) showed that S-velocities are 2-3 % lower than global average above a depth of 300 km beneath the OJP.
In this study we investigated upper mantle structure beneath the OJP by using PP-P differential travel times for PP waves of which bounce points are located on the OJP and the surrounding region. We analyzed waveform data of events from 2012 to 2013 recorded by IRIS and F-net stations.
We follow a method of Obayashi et al. (2004) to obtain PP-P differential travel time residuals. First a band-pass filter from 5 to 10 second was applied to the waveform data. To calculate PP-P differential residuals, we synthesized PP waves from P waves by applying the Hilbert transform, attenuation operator, and multi reflection/conversion effect in the crust beneath the bounce points. To calculate the multi reflection/conversion effect, we used crust structure model CRUST1.0 (REFERENCE). We then calculated PP-P differential residuals with respect to differential times predicted from the iasp91 model (Kennett and Engdahl, 1991) by cross-correlation of the observed and synthetic PP waves. Distribution of the obtained PP-P differential residuals indicated that the residuals are consistently negative for PP waves of which bounce points are located on the OJP. The average PP-P residual for such PP-waves is -1.6 second, which suggests P-velocities faster than that of iasp91 beneath the OJP, while we cannot constrain a depth range of the fast anomalies from the present study. Assuming that the average residual is due to uniformly fast structure above a depth of 300 km, P-wave velocity beneath the OJP is 1.7% faster than that of the iasp91 model.

Keywords: Ontong Java Plateau, body wave

Mechanical coupling between the plate and lowermost mantle controlled by the subducted lithosphere strength

*Tomoeki Nakakuki[1], Takeo Kaneko[1], Daisuke Yamazaki[2]

1. Department of Earth and Planetary Systems Science, Graduate School of Science, Hiroshima University, 2. Institute for Planetary Materials, Okayama University

Hotspot volcanoes are regarded as an indication of mantle plumes that originate from the deep mantle. Relative migration between the hotspot tracks suggests much slower horizontal motion of the deep mantle layer than that of the surface plates. Viscosity increase in the lower mantle is often attributed to the cause of the slow motion in the deep mantle. Numerical modeling on subducted lithospheres integrated into a mantle convection system showed that the lithosphere penetrating into the lower mantle is not assimilated thermally to the surrounding mantle, so that the subducted lithosphere should work as a substance to transmit viscous stress from the deep mantle. This implies that motion of the deep mantle layer is strongly coupled with that of the surface plate.

We performed numerical simulation of an integrated lithosphere-mantle convection system in which the subducted lithosphere penetrates into the core-mantle boundary region. We investigated effects of yield strength and viscosity reduction due to the grain-size reduction or interconnection of ferro-periclase generated at the 660-km phase transition. The viscosity in the lower mantle was controlled as the value fit to the range inferred from geoid anomalies. In addition to them, depth-dependent thermal expansivity was also considered.

When the viscosity reduction is not incorporated, viscous resistance in the deepest mantle substantially controls the lithosphere motion in the case with the yield strength of 300 MPa. The large yield strength causes that the plate motion averaged in time is maintained to be less than 5 cm/yr, except in the cases with the viscosity of the lowermost mantle less than 10^{22} Pa s. Furthermore, the horizontal motion in the lowermost region is equivalent to half value of that of the surface plate. When the yield strength is set to 200 MPa, the viscosity increase in the lower mantle generates periodic slab folds by sharp bending. This substantially absorbs difference in the motion between the surface and the lowermost mantle. The slab folding generates a lump of the subducted lithosphere, which has large negative buoyancy. Toppling of the slab lump colliding the core-mantle boundary induces episodic acceleration of the slab descent motion. At this time, the plate motion exceeds 10 cm/yr. The slab is regarded as a stress guide between the surface and lowermost mantle in spite of the deformation. The slab interaction with the CMB region would therefore appear to the surface as significant fluctuation of the plate motion. Although the slab folds are generated when the depth-dependent thermal expansivity is introduced with the yield strength of 300 MPa, the decoupling between the surface and lowermost mantle motion is not enough to explain the stationary hotspot.

When viscosity reduction beneath the 660-km phase boundary is introduced, the viscous resistance of the deep mantle is not transmitted to the surface. The viscosity of the uppermost lower mantle controls the speed of the plate motion in the range of 5 to 10 cm/yr, which is consistent with the observation. On the contrary, the speed of the deep mantle flow is reduced to about 1/5 of the surface plate motion. Slab deformation induced by the viscosity reduction is therefore an important mechanism to weaken the coupling between the plate and deep mantle and to regulate subducting plate motion.

Keywords: mantle convection, plate motion, lower mantle, subducted slab, rheology

Detection of Hadean crustal material in the deep Earth and Moon

*Dapeng Zhao[1], Yukio Isozaki[2], Shigenori Maruyama[3]

1. Department of Geophysics, Tohoku University, 2. Department of General System Studies, The University of Tokyo, 3. Earth-Life Science Institute, Tokyo Institute of Technology

Because of the tectonic erosion associated with plate subductions, the Hadean crustal material may have been brought down to the deep interior of the Earth (Kawai et al., 2009, 2013; Isozaki et al., 2010; Dohm and Maruyama, 2015; Maruyama and Ebisuzaki, 2017; Maruyama et al., 2017). The primordial material may have physical properties different from those of the surrounding mantle rocks, hence it could be detected using seismic tomography.

Significant lateral variations of S-wave velocity (Vs) are revealed in the lunar mantle by tomographic imaging (Zhao et al., 2008, 2012). A correlation between the Vs tomography and the thorium abundance distribution is found. The area with a high thorium abundance exhibits a distinct low Vs zone which extends down to a depth of ~300 km below the Procellarum KREEP Terrane (PKT), which may reflect a thermal and compositional anomaly beneath the PKT. The distribution of deep moonquakes shows a correlation with the tomography in the deep lunar mantle, similar to earthquakes which are affected by structural heterogeneities in the terrestrial crust and upper mantle. The occurrence of deep moonquakes and seismic-velocity heterogeneities implies that the lunar interior may contain a certain amount of fluids and so still be thermally and dynamically active at present. Because there is no plate tectonics in the Moon, the Hadean crustal material may have been preserved near the lunar surface till today. However, due to the mantle overturn that happened at the early stage of the Moon, part of the Hadean crustal KREEP material may have sunk to the deep mantle, which may have become heat sources for the lunar mantle activities and so caused the deep moonquakes around them.

The processes happened in the Moon may have also taken place in the deep Earth. Due to the plate subductions, the Hadean crustal KREEP material may have sunk to the deep mantle of the Earth, which may have become heat sources for mantle plumes and super-plumes. Prominent low seismic-velocity (low-V) anomalies are clearly revealed in the deep mantle beneath the surface hotspot regions such as south-central Pacific, East Africa, Hawaii and Iceland (Zhao et al., 2013; Zhao, 2015). Some of the low-V anomalies could be caused by the Hadean crustal KREEP material.

References

Dohm, J.M., S. Maruyama (2015) Habitable trinity. *Geoscience Frontiers* 6, 95-101.

Isozaki, Y., K. Aoki, T. Nakama, S. Yanai (2010) New insight into a subduction-related orogen: A reappraisal of the geotectonic framework and evolution of the Japanese Islands. *Gondwana Res.* 18, 82-105.

Kawai, K., T. Tsuchiya, J. Tsuchiya, S. Maruyama (2009) Lost primordial continents. *Gondwana Res.* 16, 581-586.

Kawai, K., S. Yamamoto, T. Tsuchiya, S. Maruyama (2013) The second continent: Existence of granitic continental materials around the bottom of the mantle transition zone. *Geoscience Frontiers* 4, 1-6.

Maruyama, S., T. Ebisuzaki (2017) Origin of the Earth: a proposal of new model called ABEL. *Geoscience Frontiers*. http://dx.doi.org/10.1016/j.gsf.2016.10.005.

Maruyama, S., M. Santosh, S. Azuma (2017) Initiation of plate tectonics in the Hadean: Eclogitization triggered by the ABEL Bombardment. *Geoscience Frontiers*. http://dx.doi.org/10.1016/j.gsf.2016.11.009.

Zhao, D. (2015) *Multiscale Seismic Tomography*. Springer, 304 pp.

Zhao, D., J. Lei, L. Liu (2008) Seismic tomography of the Moon. *Chinese Sci. Bull.* 53, 3897-3907.

Zhao, D., T. Arai, L. Liu, E. Ohtani (2012) Seismic tomography and geochemical evidence for lunar mantle heterogeneity: Comparing with Earth. *Global Planet. Change* 90, 29-36.
Zhao, D., Y. Yamamoto, T. Yanada (2013) Global mantle heterogeneity and its influence on teleseismic regional tomography. *Gondwana Res.* 23, 595-616.

Keywords: Hadean crust, moonquake, seismic tomography, KREEP, thorium

Grain growth kinetics in pyrolite composition: Implications for grain-size evolution of lower-mantle slab

*Masahiro Imamura[1], Tomoaki Kubo[1]

1. Kyushu University

Viscosity of lower-mantle slab largely depends on grain size in constituent minerals. It consists of bridgmanite (Brg), ferro-periclase (Fp), Ca-perovskite (Capv), and majoritic garnet (Mjgt) in the case of pyrolite composition. The grain-size evolution of lower-mantle slab is mainly controlled by grain growth process after the significant grain-size reduction due to the post-spinel transformation. Grain growth kinetics can be described by $d^n-d_0^n=kt$ (d: grain size, d_0: initial grain size,n: grain growth exponent, k: Arrhenius-type rate constant, t: time). In the multiphase system, Zener pinning is an important process and grain growth of the primary phase is controlled by Ostwald ripening of the secondary phase, which can be described by $d_I/d_{II}=\beta/f_{II}^z$ (d_I: grain size of primary phase, d_{II}: grain size of secondary phase, f_{II}: volume fraction of secondary phase, β and z: Zener parameters). In the present study, we conducted grain growth experiments in pyrolite composition under lower mantle conditions, and discuss the grain-size evolution of lower-mantle slab.

Annealing experiments in pyrolitic material were conducted at 25-27 GPa and 1600-1950˚C for 30-3000 min using a Kawai-type apparatus at Kyushu University. FE-SEM was used for microstructural observations and chemical analysis. Four phases of Brg (~70 vol%), Fp (~15 vol%), Mjgt (~13 vol%), and Capv (~2 vol%) were observed in recovered samples annealed at 25 GPa. To avoid the effects of the eutectoid texture on the kinetics, we took the grain growth data only from the sample exhibiting relatively homogeneous polygonal texture. Both secondary phases of Fp and Mjgt are homogeneously distributed in the Brg-dominant sample after the polygonal texture was achieved. The grain size ratio of d_{Brg}/d_{Fp} and d_{Brg}/d_{Mjgt} are almost constant during the grain growth and estimated to be ~1.7 and ~1.2, respectively. These microstructural observations imply that the Brg grain growth is pinned by the secondary phases, and the rate is controlled by Ostwald ripening kinetics. We obtained n values of 6.2, 3.3, and 3.1 for Brg, Fp, and Mjgt, respectively. The averaged n value of ~4.2 is consistent with the multiphase grain growth model when the secondary phase grows by Ostwald ripening process (n=4, grain-boundary diffusion controlled). When assuming the n-value of 4, the activation enthalpies for Brg, Fp, and Mjgt are estimated to be ~410, ~240, and ~500 kJ/mol, respectively, implying that the rate-controlling species are different between Ostwald ripening processes of Fp and Mjgt, and the Brg grain growth is controlled by both processes. If we treat Fp and Mjgt as a secondary phase ($d_{II=Fp+Mjgt}$) ignoring Capv, the activation enthalpies are almost the same between the primary and secondary phases. The grain size ratio of $d_{I=Brg}/d_{II=Fp+Mjgt}$ is ~1.5 with the $f_{II=Fp+Mjgt}$ of 0.3, which is almost consistent with the previous systematic study in the olivine-enstatite system (Tasaka and Hiraga, 2013). On the other hand, three phases without Mjgt were present at higher pressure of 27 GPa, in which the grain size was slightly larger probably due to the smaller proportion of the secondary phases (~77 vol% of Brg).

On the basis of the results obtained above, we estimated grain-size evolution of lower-mantle slab assuming that Zener parameters are the same as the previous study (Tasaka and Hiraga, 2013). The grain size of Brg in a pyrolitic composition with ($f_{II=Fp+Mjgt}$=0.3) and without ($f_{II=Fp}$=0.2) bearing Mjgt is estimated to be ~5-650 μm and ~50-900 μm, respectively, at 800-1600˚C in 10^8 years. When considering an olivine-like ($f_{II=Fp}$=0.3) and a perovskitic ($f_{II=Fp}$=0.1) compositions, the Brg grain size decreases to ~40-720 μm and increases to ~80-1270 μm, respectively. Thus, the grain size in lower-mantle slab is likely kept smaller than 1 mm, suggesting that grain-size sensitive creep is dominant. Viscosity variations in lower-mantle slab will be discussed considering a dynamic grain-growth effect.

A revisit on initial temperature at the core-mantle boundary in a coupled core-mantle evolution model

*Takashi Nakagawa[1]

1. MAT, JAMSTEC

An initial temperature at the core-mantle boundary (CMB) is an important constraint for thermal evolution of Earth’s mantle and core because this temperature strongly affects the size and onset timing of growing inner core, primordial heat in early Earth’s core and thermal and chemical state in the deep mantle. In a previous study, we found ~6000 K as the initial CMB temperature in a coupled core-mantle evolution model to match constraints of thermal evolution of Earth’s core [Nakagawa and Tackley, 2010]. However, in recent suggestions from high P-T physics and theoretical model of thermal evolution of Earth’s core, the initial CMB temperature seems to be less than ~5000 K [Andrault et al., 2016; Nakagawa, in revisoin]. Since our core evolution model is based on a simplified analytical formulation [Buffett et al., 1992; Buffett et al., 1996] and more complicated formulation that can fit the density structure derived from seismological analysis and applicable for high thermal conductivity of iron alloy is proposed [Labrosse, 2015], we reassess the initial CMB temperature that can find the best-fit core evolution scenario. Because of thermostat effects on thermal evolution [e.g. Nakagawa and Tackley, 2010; Nakagawa and Tackley, 2012], the initial CMB temperature may not be sensitive to the scenario of thermal evolution of Earth’s core and mantle but the heat flow across the CMB found in this study (9 to 10 TW) is slightly lower than the lower-bound value (11 TW). On the magnetic evolution, the low thermal conductivity is still more preferable than high thermal conductivity due to existence of adiabatic shell with high thermal conductivity that suppress a convective region of Earth’s core. In the presentation, we will attempt to an implication for detectability of geoneutrino based on thermal and chemical evolution modeling of Earth’s mantle and core.

Keywords: core-mantle boundary temperature, thermal evolution, Earth's metallic core

